Circulation Research
JOURNAL OF THE AMERICAN HEART ASSOCIATION

AKAP150 Contributes to Enhanced Vascular Tone by Facilitating Large-Conductance Ca^{2+}-Activated K^+ Channel Remodeling in Hyperglycemia and Diabetes Mellitus

Matthew A. Nystoriak, Madeline Nieves-Cintrón, Patrick J. Nygren, Simon A. Hinke, C. Blake Nichols, Chao-Yin Chen, Jose L. Puglisi, Leighton T. Izu, Donald M. Bers, Mark L. Dell'Acqua, John D. Scott, Luis F. Santana and Manuel F. Navedo

Circ Res. 2014;114:607-615; originally published online December 9, 2013;
doi: 10.1161/CIRCRESAHA.114.302168
Circulation Research is published by the American Heart Association, 7272 Greenville Avenue, Dallas, TX 75231

Print ISSN: 0009-7330. Online ISSN: 1524-4571

AKAP150 Contributes to Enhanced Vascular Tone by Facilitating Large-Conductance Ca^{2+}-Activated K^+ Channel Remodeling in Hyperglycemia and Diabetes Mellitus

Matthew A. Nystoriak, Madeline Nieves-Cintrón, Patrick J. Nygren, Simon A. Hinke, C. Blake Nichols, Chao-Yin Chen, Jose L. Puglisi, Leighton T. Izu, Donald M. Bers, Mark L. Dell'Acqua, John D. Scott, Luis F. Santana, Manuel F. Navedo

Rationale: **Increased contractility of arterial myocytes and enhanced vascular tone during hyperglycemia and diabetes mellitus may arise from impaired large-conductance Ca^{2+}-activated K^+ (BK_{Ca}) channel function. The scaffolding protein A-kinase anchoring protein 150 (AKAP150) is a key regulator of calcineurin (CaN), a phosphatase known to modulate the expression of the regulatory BK_{Ca} β1 subunit. Whether AKAP150 mediates BK_{Ca} channel suppression during hyperglycemia and diabetes mellitus is unknown.**

Objective: **To test the hypothesis that AKAP150-dependent CaN signaling mediates BK_{Ca} β1 downregulation and impaired vascular BK_{Ca} channel function during hyperglycemia and diabetes mellitus.**

Methods and Results: **We found that AKAP150 is an important determinant of BK_{Ca} channel remodeling, CaN/nuclear factor of activated T-cells c3 (NFATc3) activation, and resistance artery constriction in hyperglycemic animals on high-fat diet. Genetic ablation of AKAP150 protected against these alterations, including augmented vasoconstriction. D-glucose–dependent suppression of BK_{Ca} channel β1 subunits required Ca^{2+} influx via voltage-gated L-type Ca^{2+} channels and mobilization of a CaN/NFATc3 signaling pathway. Remarkably, high-fat diet mice expressing a mutant AKAP150 unable to anchor CaN resisted activation of NFATc3 and downregulation of BK_{Ca} β1 subunits and attenuated high-fat diet–induced elevation in arterial blood pressure.**

Conclusions: **Our results support a model whereby subcellular anchoring of CaN by AKAP150 is a key molecular determinant of vascular BK_{Ca} channel remodeling, which contributes to vasoconstriction during diabetes mellitus. (*Circ Res*. 2014;114:607-615.)**

Key Words: calcineurin ■ hyperglycemia ■ hypertension ■ ion channels ■ potassium channels

Vascular complications associated with noninsulin-dependent (type 2) diabetes mellitus contribute to hypertension, heart disease, stroke, and retinal degeneration.[1] Although the cellular mechanisms of vascular dysfunction in patients with diabetes mellitus are complex and poorly understood, elevated intracellular Ca^{2+} and enhanced contractility of arterial myocytes lining the resistance vasculature represent a major contributing factor.[2,3]

Editorial, see p 588

Arterial myocyte contractility is predominantly controlled by membrane potential (V_M) and Ca^{2+} entry via voltage-gated L-type Ca^{2+} channels (LTCCs). The opening of a single or small cluster of these channels produces a localized elevation in intracellular Ca^{2+} or sparklet near the plasma membrane.[4] Ca^{2+} sparklet activity increases in arterial myocytes during acute hyperglycemia and diabetes mellitus.[5] Although this increase in LTCC-mediated Ca^{2+} influx directly enhances myocyte contractility, sustained activity could also potentially drive Ca^{2+}-dependent changes in gene expression during diabetes mellitus via activation of the Ca^{2+}/calmodulin-dependent phosphatase calcineurin (CaN) and subsequent dephosphorylation and nuclear translocation of the transcription factor nuclear factor of activated T-cells c3 isoform (NFATc3).[6,7] CaN is anchored at the plasma membrane in close proximity to LTCCs by A-kinase anchoring protein (AKAP) 150 (murine ortholog of human AKAP79),[8] which is required for activation of CaN-NFAT signaling.[9] Disruption

Original received July 9, 2013; revision received December 5, 2013; accepted December 9, 2013. In November 2013, the average time from submission to first decision for all original research papers submitted to *Circulation Research* was 14.6 days.

From the Department of Pharmacology, University of California, Davis (M.A.N., M.N.-C., C.B.N., C.-Y.C., J.L.P., L.T.I., D.M.B., M.F.N.); Department of Pharmacology, University of Colorado, Denver (M.L.D.); Department of Pharmacology, Howard Hughes Medical Institute, University of Washington, Seattle, WA (P.J.N., S.A.H., J.D.S.); and Department of Physiology and Biophysics, University of Washington, Seattle (L.F.S.).

The online-only Data Supplement is available with this article at http://circres.ahajournals.org/lookup/suppl/doi:10.1161/CIRCRESAHA.114.302168/-/DC1.

Correspondence to Manuel F. Navedo, PhD, Department of Pharmacology, University of California, One Shields Ave, Davis, CA 95616. E-mail mfnavedo@ucdavis.edu

Nonstandard Abbreviations and Acronyms

AKAP150	A-kinase anchoring protein 150
BK_{Ca}	large-conductance Ca^{2+}-activated potassium channel
BK_{Ca} β1	BK_{Ca} β 1 subunit
CaN	calcineurin
CsA	cyclosporine A
EGFP	enhanced green fluorescent protein
HFD	high-fat diet
IbTx	iberiotoxin
LTCC	L-type Ca^{2+} channel
NFATc3	nuclear factor of activated T-cells c3 isoform
ΔPIX	AKAP150 lacking binding site for calcineurin
Po	open probability
V_M	membrane potential
WT	wild type

of the interaction between CaN and AKAP150 precludes subplasmalemmal CaN localization and CaN-dependent NFAT transcriptional activation in rat hippocampal neurons.[10] However, the importance of AKAP150 in the modulation of vascular gene expression and vascular tone during diabetes mellitus is unknown.

Activation of CaN/NFATc3 in arterial myocytes is linked to the expression of large-conductance Ca^{2+}-activated K^+ (BK_{Ca}) channels,[11,12] which provide tonic feedback opposition to membrane depolarization and LTCC activation in arterial myocytes.[13] In these cells, BK_{Ca} channels are composed of pore-forming α subunits in association with accessory β1 subunits.[14] Loss of the β1 subunit results in decreased Ca^{2+} sensitivity, reduced BK_{Ca} activation, and increased vascular tone.[15]

The objective of the present study was to examine the role of AKAP150-dependent signaling in BK_{Ca} channel remodeling and vascular dysfunction during hyperglycemia and diabetes mellitus. Our hypotheses were tested in high-fat diet (HFD)–fed mice, a well-suited mouse model for the study of pathophysiology associated with induction of type 2 diabetes mellitus.[16,17] We found that BK_{Ca} β1 subunit (BK_{Ca} β1) expression is suppressed, leading to reduced BK_{Ca} channel Ca^{2+} sensitivity and enhanced vasoconstriction in wild-type (WT) but not in AKAP150-null ($AKAP150^{-/-}$) high-fat mice. This effect was dependent on LTCC-mediated Ca^{2+} influx and CaN/NFATc3 activation. Furthermore, we discovered that disruption of the interaction between AKAP150 and CaN was equally effective in preventing β1 suppression and NFATc3 activation and attenuated increases in blood pressure in HFD mice. These results implicate AKAP150 as an essential component of BK_{Ca} suppression, thus contributing to enhanced vascular tone during type II diabetes mellitus.

Methods

WT (C57Bl/6J, BalbC), $AKAP150^{-/-}$ (C57Bl/6J), $NFATc3^{-/-}$ (BalbC), and knock-in mice expressing AKAP150 lacking its CaN-binding site (ΔPIX)[16] were euthanized by intraperitoneal injection of sodium pentobarbital as approved by the University of California, Davis Institutional Animal Care and Use Committee. Mice were placed on either a low-fat diet (10% kcal; control) or HFD (60% kcal; Research Diets) at 5 weeks of age and were sustained for 24 to 26 weeks. The composition of these diets and the propensity of mice maintained on this HFD to develop type 2 diabetes mellitus have been described previously.[18] For some experiments, cerebral and mesenteric arteries were acutely isolated from ct animals (5 weeks of age) and organ cultured by placing arteries in serum-free DMEM-F12 culture media (Thermo Scientific) with varying concentrations of D-glucose and incubating at 37°C and 5% CO_2 for 48 hours. Arterial myocytes were dissociated from cerebral and mesenteric arteries using enzymatic digestion techniques described previously.[11] Vascular tone was measured using an IonOptix Vessel Diameter system. Currents were recorded using an Axopatch 200B amplifier. Images were obtained using a confocal microscope. Data are presented as mean±SEM. $P<0.05$ was considered statistically significant, which is denoted by an asterisk in the figures. An expanded Methods section is available in the online-only Data Supplement.

Results

Our hypotheses were tested using freshly isolated arteries and arterial myocytes from age-matched WT and $AKAP150^{-/-}$ mice fed an ad libitum supply of either a low-fat diet (10% kcal) or HFD (60% kcal; see Methods for details).[18] We used this model because it closely recapitulates features of clinically relevant human pathology in type 2 diabetes mellitus.[17,18] Furthermore, it does not depend on genetic manipulation or chemical destruction of pancreatic β-cells. Nonfasting blood glucose and body mass were significantly higher in HFD mice compared with low-fat diet–fed (ct) mice (Online Table I). Genetic ablation of AKAP150 did not affect nonfasting blood glucose levels in ct or HFD mice compared with corresponding WT ct (Online Table I).

Impaired Arterial Tone and Iberiotoxin Sensitivity in WT But Not in $AKAP150^{-/-}$ HFD Mice

At the physiological intravascular pressure of 60 mm Hg,[19] WT HFD arteries were consistently more constricted than WT ct (29±4% versus 17±2% vascular tone, respectively; Figure 1A and 1B). To evaluate the contribution of BK_{Ca} channels to the regulation of arterial tone, the selective BK_{Ca} inhibitor iberiotoxin (IbTx; 100 nmol/L) was applied to the bath solution. Whereas application of IbTx caused marked constriction in WT ct arteries (13±4% decrease in diameter), this agent had little effect on WT HFD vessels (2±2% decrease in diameter; Figure 1A–1C).

We determined whether the anchoring protein AKAP150 mediates decreased IbTx sensitivity in HFD arteries. To do this, we examined tone development and IbTx-induced constriction in $AKAP150^{-/-}$ ct and HFD-isolated arteries. In contrast to WT arteries, levels of arterial tone and IbTx-induced constriction were similar in $AKAP150^{-/-}$ ct and HFD vessels (Figure 1A–1C). Arteries from all groups responded with robust constriction to phenylephrine (Online Figure I), suggesting that altered IbTx responses between groups were not because of differences in the magnitude of baseline tone development. Constriction was significantly greater in the presence of phenylephrine in WT HFD but not in $AKAP150^{-/-}$ HFD arteries (compared with respective ct). Enhanced vascular tone was not a result of increased expression of L-type Ca^{2+} channels because basal expression of the pore-forming subunit $Ca_V1.2$ was similar between WT and $AKAP150^{-/-}$ ct and HFD arteries (Online Figure II). These

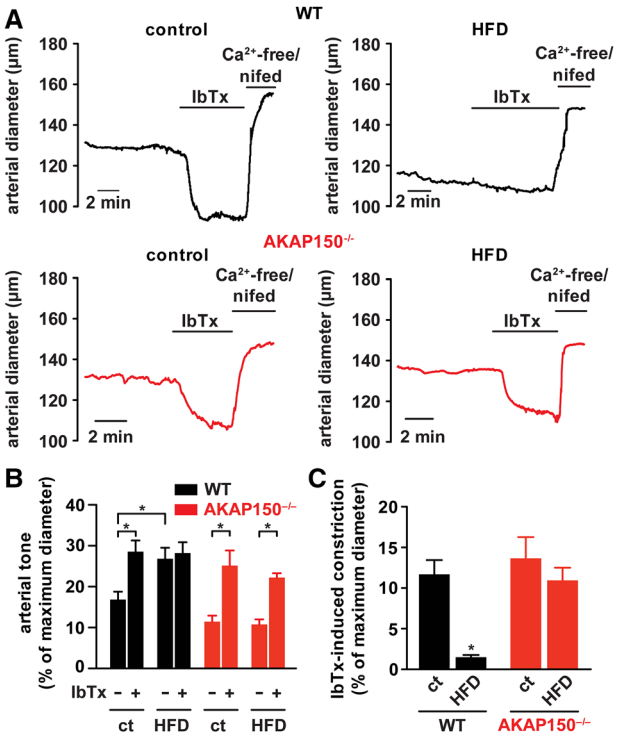

Figure 1. A-kinase anchoring protein 150 (AKAP150) is necessary for enhanced arterial tone and diminished iberiotoxin-sensitive constriction in high-fat diet (HFD) arteries. **A**, Representative diameter recordings from pressurized (60 mm Hg) wild-type (WT) and AKAP150$^{-/-}$ control (ct) and HFD cerebral arteries before and after iberiotoxin (IbTx; 100 nmol/L). Bar plot of vascular tone (in the absence [–] and presence [+] of IbTx; **B**) and IbTx-induced constriction (**C**) at 60 mm Hg in WT ct (n=8 from 6 animals), WT HFD (n=6 from 5 animals), AKAP150$^{-/-}$ ct (n=7 from 5 animals), and AKAP150$^{-/-}$ HFD (n=8 from 5 animals) arteries (*P<0.05).

data suggest impaired BK_{Ca} channel function and support the hypothesis that enhanced vasoconstriction in HFD mice requires AKAP150.

AKAP150 Is Required for Downregulation of BK_{Ca} β1 Subunits During Diabetes Mellitus

We tested the possibility that reduced BK_{Ca}-mediated regulation of vascular tone in WT HFD results from altered Ca^{2+} sparks, which are the physiological activators of BK_{Ca} channels in arterial myocytes.[20] To do this, we optically measured Ca^{2+} sparks in freshly isolated cerebral arterial myocytes loaded with the Ca^{2+}-sensitive dye fluo-4 using spinning disk confocal microscopy. As shown in Online Figure III, the frequency and amplitude Ca^{2+} sparks were similar in WT ct, WT HFD, and AKAP150$^{-/-}$ HFD myocytes, suggesting that changes in Ca^{2+} spark activity do not underlie impaired BK_{Ca} function in WT HFD mice.

Next, we recorded single BK_{Ca} channel currents from WT and AKAP150$^{-/-}$ arterial myocytes using the inside-out configuration of the patch clamp technique to determine whether AKAP150 mediates impairment of BK_{Ca} channel function during diabetes mellitus. Currents were recorded at physiological V_M (–40 mV) in the presence of 1 and 10 µmol/L free Ca^{2+}. Although the open probability (P_o) of BK_{Ca} channels increased when Ca^{2+} was elevated from 1 to 10 µmol/L in myocytes from both groups, BK_{Ca} channel P_o from WT HFD was significantly lower than that from WT ct at the Ca^{2+} concentrations tested (Figure 2A and 2B). Consistent with arterial diameter data above, P_o for BK_{Ca} channels was similar in AKAP150$^{-/-}$ ct and HFD cells (Figure 2A and 2B). Open time histograms for BK_{Ca} channels from WT and AKAP150$^{-/-}$ cells are shown in Figure 2C. Histograms were fit with a sum of 2 Gaussian functions (see Methods for details) and revealed a shift toward shorter open times in WT HFD compared with WT ct. Open times were not different for BK_{Ca} channels from AKAP150$^{-/-}$ HFD and ct cells. These results indicate that AKAP150 is required for a reduction in Ca^{2+} sensitivity and dwell open time of BK_{Ca} channels during diabetes mellitus.

Reduced Ca^{2+} sensitivity and open time of BK_{Ca} channels in WT HFD cells are consistent with downregulation of the β1 subunit.[15] Accordingly, we found that application of 1 µmol/L tamoxifen, which increases BK_{Ca} channel P_o through the regulatory β1 subunit (Online Figure IV),[21] significantly increased the P_o of BK_{Ca} channels from WT ct (5-fold) but had minimal effect in WT HFD cells (Figure 3A and 3B). In contrast, tamoxifen increased BK_{Ca} channel P_o from AKAP150$^{-/-}$ ct and HFD myocytes, which suggests restored β1 function (Figure 3A and 3B). Consistent with the data above, Western blot analysis showed ≈65% reduction in BK_{Ca} β1 protein in lysates from WT HFD but not from WT and AKAP150$^{-/-}$ ct and AKAP150$^{-/-}$ HFD (Figure 3C and 3D). Expression of the

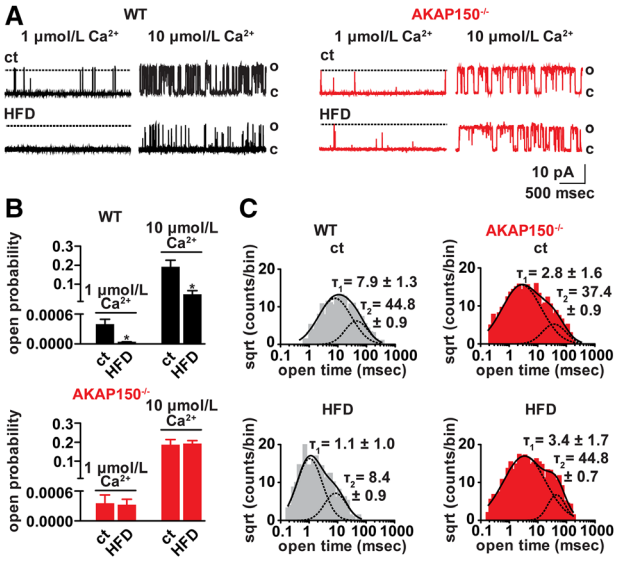

Figure 2. A-kinase anchoring protein 150 (AKAP150) is necessary for reduced large-conductance Ca^{2+}-activated K^+ (BK_{Ca}) channel Ca^{2+} sensitivity and dwell open time in high-fat diet (HFD) arterial myocytes. **A**, Representative single BK_{Ca} channel records at –40 mV obtained from excised membrane patches of isolated wild-type (WT) and AKAP150$^{-/-}$ control (ct) and HFD arterial myocytes in the presence of 1 and 10 µmol/L free Ca^{2+} bath solution (C: closed; O: open). **B**, Bar plot summarizing BK_{Ca} channel open probability (P_o) at indicated free Ca^{2+} concentrations from WT ct (n=11 from 5 mice) and HFD (n=11 from 6 mice) and AKAP150$^{-/-}$ ct (n=17 from 6 mice) and HFD (n=10 from 6 mice) cells. **C**, Open dwell time histograms for BK_{Ca} channels in WT and AKAP150$^{-/-}$ ct and HFD arterial myocytes. Black lines represent best fit to data with a 2-component Gaussian function with centers at indicated values (τ; ms; R^2>0.90; *P<0.05).

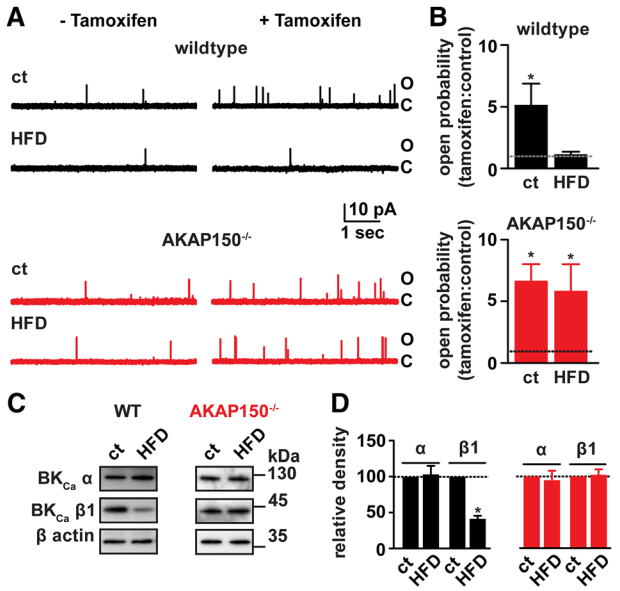

Figure 3. A-kinase anchoring protein 150 (AKAP150) is necessary for impaired large-conductance Ca^{2+}-activated K^+ (BK_{Ca}) β1 subunit function and downregulation of β1 subunit expression in high-fat diet (HFD) arterial myocytes. **A**, Exemplar single BK_{Ca} channel records at –40 mV and 1 μmol/L Ca^{2+} obtained from excised membrane patches of isolated wild-type (WT) and AKAP150$^{-/-}$ control (ct) and HFD myocytes in the presence and absence of tamoxifen (1 μmol/L). **B**, Bar plots summarizing open probability (P_o; tamoxifen:control) from WT ct (n=9 from 4 mice), WT HFD (n=9 from 3 mice), AKAP150$^{-/-}$ ct (n=9 from 4 mice), and AKAP150$^{-/-}$ HFD (n=8 from 4 mice) myocytes. *P<0.05 (1 sample t test using hypothetical value=1.0). Representative Western blots (**C**) and corresponding densitometric summary data (**D**) for BK_{Ca} α and β1 subunits in WT ct (n=6) and HFD (n=8) and AKAP150$^{-/-}$ ct (n=5) and HFD (n=5) arteries.

pore-forming BK_{Ca} α subunit was unchanged between groups (Figure 3C and 3D). Note that ablation of AKAP150 did not alter basal expression of BK_{Ca} subunits (Online Figure VA). Furthermore, no change in channel density was observed because the number of functional channels in membrane patches (HFD: 4.0±1.0; control: 4.0±0.4) and current–voltage relationship of whole-cell, IbTx-sensitive potassium currents (ie, I_{BK}; Online Figure VI) were not different between WT and AKAP150$^{-/-}$ groups. Together, these data indicate that AKAP150 mediates downregulation of BK_{Ca} β1 subunits and decreases channel function in diabetic mice.

Elevation of Extracellular Glucose Recapitulates AKAP150-Dependent Suppression of BK_{Ca} Channel Function and β1 Subunit Expression

To isolate the effects of glucose from confounding conditions that may be present in HFD mice (eg, circulating agents, hypercholesterolemia, intravascular pressure), arteries were isolated and preincubated for 48 hours in media containing 5, 10, or 20 mmol/L D-glucose. These extracellular D-glucose concentrations are within the range of observed nonfasting blood glucose levels reported for HFD (20 mmol/L) and control mice (5–10 mmol/L; Online Table I). Basal expression of BK_{Ca} channel subunits in vessels maintained under normoglycemic conditions (eg, 5 and 10 mmol/L D-glucose) was similar to that in freshly isolated WT ct arteries (Online Figure VB).

BK_{Ca} channel P_o in myocytes from arteries incubated in 5 or 10 mmol/L D-glucose was similar in bath solutions containing 1 and 10 μmol/L Ca^{2+} (Figure 4). BK_{Ca} channel P_o observed under these conditions was similar to that in myocytes from nondiabetic control mice (Figure 2B). In contrast, the P_o of BK_{Ca} channels in myocytes from WT arteries maintained in 20 mmol/L D-glucose was significantly reduced (Figure 4). This reduction in BK_{Ca} channel P_o was not observed in cells from arteries incubated in 20 mmol/L D-glucose when the LTCC antagonist nifedipine (1 μmol/L) or diltiazem (50 μmol/L) was present in the incubation media or when mannitol (15 mmol/L; a stable and nonpermeable monosaccharide) or the nonmetabolized L-glucose (15 mmol/L) was substituted for D-glucose (Figure 4; Online Figure VII). BK_{Ca} channel P_o was similar between AKAP150$^{-/-}$ myocytes incubated in 10 (chosen as the normoglycemic control) or 20 mmol/L D-glucose at both Ca^{2+} concentrations examined (Figure 4). Consistent with functional data, no difference in β1 transcript and protein levels was observed in WT arteries incubated in 5 or 10 mmol/L D-glucose (Online Figure VIII). Raising D-glucose to 20 mmol/L did not change α subunit protein levels but caused >50% reduction in β1 transcript and protein in WT arteries, which was prevented by nifedipine and ablation of AKAP150$^{-/-}$ (Online Figure VIII). Together, these data suggest that hyperglycemic conditions

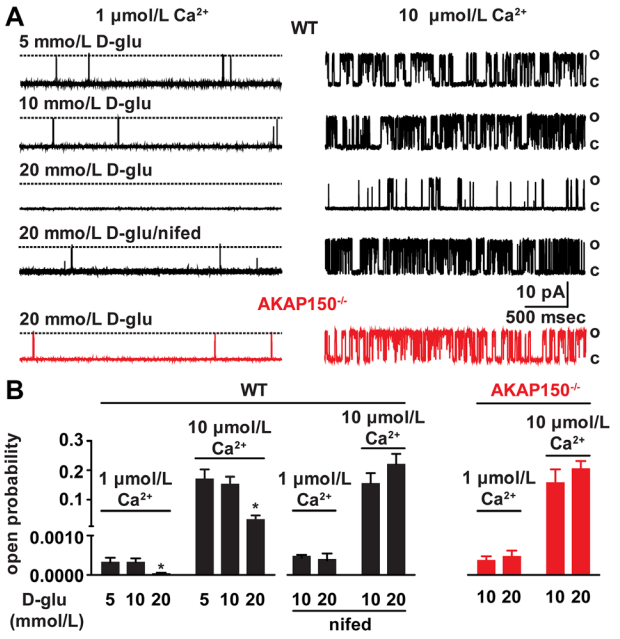

Figure 4. Nifedipine and ablation of A-kinase anchoring protein 150 (AKAP150) prevent decreased large-conductance Ca^{2+}-activated K^+ (BK_{Ca}) channel function by elevated glucose. **A**, Exemplar single BK_{Ca} currents recorded from excised membrane patches of myocytes isolated from wild-type (WT) and AKAP150$^{-/-}$ cerebral arteries incubated (48 hours) in specified D-glucose concentration in the presence and absence of nifedipine (1 μmol/L) at –40 mV and in the presence of 1 and 10 μmol/L free Ca^{2+} bath solution, (C: closed; O: open). **B**, Bar plot summarizing BK_{Ca} channel open probability (P_o) in myocytes from WT arteries incubated in the presence of 5 (n=8 cells), 10 (n=7 cells), and 20 mmol/L (n=8 cells) D-glucose and 10 (n=11 cells) and 20 mmol/L (n=11 cells) D-glucose+nifedipine and from AKAP150$^{-/-}$ arteries incubated in 10 (n=12 cells) and 20 mmol/L (n=11 cells) D-glucose at indicated Ca^{2+} concentrations (*P<0.05).

recapitulate downregulation of BK_{Ca} channel activity and β1 subunit expression observed in HFD mice. Furthermore, D-glucose–induced suppression of vascular β1 subunit expression and BK_{Ca} channel function are dependent on Ca^{2+} influx via LTCCs and AKAP150.

Anchoring of CaN by AKAP150 Is Required for BK_{Ca} Channel Impairment During Hyperglycemia and Diabetes Mellitus

Expression of BK_{Ca} channel β1 subunits in smooth muscle is modulated by Ca^{2+}/calmodulin-dependent activation of the CaN/NFATc3 pathway.[12] Supporting a role for this pathway in BK_{Ca} β1 suppression during hyperglycemia and diabetes mellitus, cellular CaN activity was significantly higher in arteries isolated from WT HFD mice (Figure 5A) and in arteries incubated in 20 mmol/L D-glucose (Online Figure IXA) compared with arteries from WT ct and incubated in 10 mmol/L D-glucose, respectively. To determine whether CaN activation plays a role in BK_{Ca} suppression, we measured single BK_{Ca} channel currents in myocytes from arteries preincubated ex vivo for 48 hours in 10 or 20 mmol/L D-glucose in the absence and presence of the CaN inhibitor cyclosporine A (CsA; 1 μmol/L), which selectively inhibits CaN activity (Online Figure IXB and IXC). Whereas arterial myocytes exhibited reduced BK_{Ca} channel P_o and β1 subunit protein expression after incubation in elevated D-glucose, channel activity and β1 expression in cells maintained in 20 mmol/L D-glucose+CsA were similar to low D-glucose ct cells from arteries incubated in the presence or absence of CsA (Figure 5B and 5C). These data indicate that CaN activation is required for the suppression of BK_{Ca} channel activity and β1 subunit expression in response to elevated extracellular D-glucose.

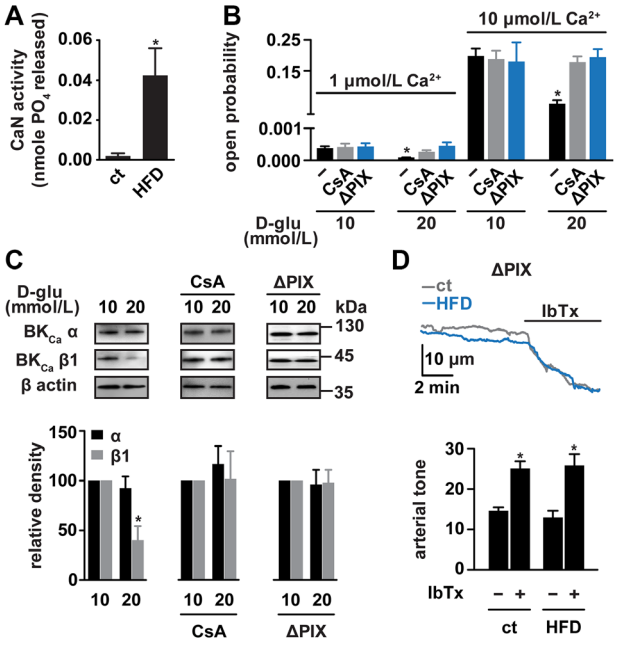

Figure 5. Anchoring of calcineurin by A-kinase anchoring protein 150 (AKAP150) is necessary for large-conductance Ca^{2+}-activated K^+ (BK_{Ca}) channel suppression and impaired vasoconstriction in response to elevated glucose and high-fat diet (HFD). A, Cellular calcineurin (CaN) activity in wild-type (WT) control (ct; n=4 from 4 animals) and HFD (n=4 from 4 animals) mesenteric arteries. **B**, Bar plot summarizing BK_{Ca} channel open probability (P_o) from WT cerebral arteries incubated in 10 and 20 mmol/L D-glucose in the absence (DMSO ct; n=11 and 10 cells, respectively) and presence of cyclosporine A (CsA; 1 μmol/L; n=10 and 6 cells, respectively). Also shown are summary data for AKAP150 lacking binding site for calcineurin (ΔPIX) arteries incubated in 10 (n=13 cells) and 20 mmol/L (n=11 cells) D-glucose. **C**, Representative Western blots (**top**) and summary densitometric data (**bottom**) showing immunoreactive bands corresponding to BK_{Ca} α and β1 subunits and β actin for WT arteries maintained in 10 and 20 mmol/L D-glucose in the absence (n=4) and presence (n=4) of 1 μmol/L CsA and ΔPIX arteries (n=5) maintained in 10 and 20 mmol/L D-glucose. **D**, Representative diameter recordings (**top**) and summary vascular tone data (**bottom**) from pressurized (60 mm Hg) ΔPIX ct (n=9 from 6 animals) and HFD (n=8 from 5 animals) cerebral arteries in the absence (–) and presence (+) of iberiotoxin (IbTx; 100 nmol/L; passive diameters for representative recordings=143 and 145 μm, respectively; *P<0.05).

Considering that AKAP150 targets CaN near the membrane, we tested whether anchoring of CaN by AKAP150 is necessary for BK_{Ca} suppression in arterial myocytes under hyperglycemic conditions. We took advantage of a knock-in mouse expressing a mutant AKAP150 lacking amino acid residues 655 to 661 of the atypical PxIxIT motif (ΔPIX), which are responsible for tethering CaN (Online Figure IXD).[16,22] No differences in basal BK_{Ca} α and β1 protein expression levels were observed between WT and ΔPIX arteries (Online Figure VA). Similar to CsA inhibition of CaN, disrupting the AKAP150/CaN interaction completely abolished the reduction in BK_{Ca} P_o and β1 subunit protein expression (Figure 5B and 5C) in response to elevated D-glucose.

To further test whether AKAP150-anchored CaN regulates BK_{Ca} channel expression during diabetes mellitus, we fed ΔPIX mice with either a control or HFD (Online Table I). Consistent with our hypothesis, BK_{Ca} channel P_o and α and β1 subunit protein expression were similar in ΔPIX ct and HFD arterial myocytes and arteries (Online Figure IXE and IXF). Furthermore, vascular tone and IbTx-induced constriction were similar in ΔPIX ct and HFD vessels (Figure 5D). These data indicate that subcellular anchoring of CaN by AKAP150 is a major determinant of signaling events regulating BK_{Ca} β1 subunit suppression and function that contribute to enhanced vasoconstriction during hyperglycemia and diabetes mellitus.

AKAP150-Dependent Anchoring of CaN Is Required for Activation of NFATc3 in Arterial Myocytes During Diabetes Mellitus

CaN dephosphorylates the transcription factor NFATc3. Once dephosphorylated, NFATc3 translocates into the nucleus of arterial myocytes and alters the expression of several genes, including BK_{Ca} β1.[12] We investigated NFATc3 localization in WT ct and HFD mesenteric artery myocytes transfected in vivo with enhanced green fluorescent protein (EGFP)–tagged NFATc3. Although WT ct demonstrates mostly cytosolic NFATc3-EGFP fluorescence, WT HFD cells exhibited NFATc3-EGFP signal localized to the nucleus (Figure 6A and 6B). However, NFATc3-EGFP nuclear translocation in $AKAP150^{-/-}$ HFD myocytes was significantly attenuated (Figure 6A and 6B). Note that WT ct and HFD myocytes expressing a construct containing only EGFP exhibited mostly cytosolic fluorescence (Online Figure X). We also examined dephosphorylation of NFATc3 serine 265, which is required for unmasking a nuclear localization signal,[23] in WT,

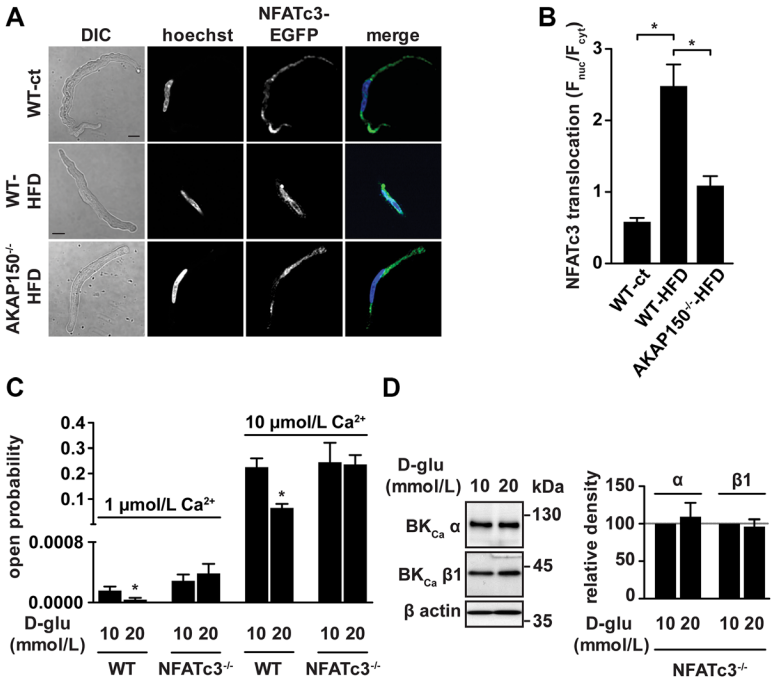

Figure 6. Activation of nuclear factor of activated T-cells c3 isoform (NFATc3) signaling is necessary for large-conductance Ca^{2+}-activated K^+ (BK_{Ca}) channel suppression in response to elevated glucose and high-fat diet (HFD) and proceeds through A-kinase anchoring protein 150 (AKAP150). **A**, Transmitted light and confocal images of ct and HFD wild-type (WT) and AKAP150$^{-/-}$ mesenteric artery myocytes expressing NFATc3-enhanced green fluorescent protein (EGFP). **B**, Bar plot summarizing NFATc3-EGFP nuclear translocation ($F_{nuclear}/F_{cytosolic}$) in WT control (ct; n=44 from 3 animals) and HFD (n=49 from 3 animals) and AKAP150$^{-/-}$ HFD (n=51 from 3 animals) myocytes. **C**, Bar plot of BK_{Ca} channel open probability (P_o) in WT (BalbC) and NFATc3$^{-/-}$ myocytes maintained in 10 (WT=6 cells; NFATc3$^{-/-}$=9 cells) or 20 mmol/L (WT=10 cells; NFATc3$^{-/-}$=11 cells) D-glucose. **D**, Representative Western blots (**top**) and corresponding densitometric summary data (**bottom**) for BK_{Ca} α and β1 subunits from NFATc3$^{-/-}$ arteries maintained in 10 and 20 mmol/L D-glucose (n=5 each; *P<0.05).

AKAP150$^{-/-}$ and ΔPIX ct, and HFD myocytes (Online Figure XI). Consistent with the activation and nuclear localization of this transcription factor in WT myocytes during hyperglycemia, we found a ≈75% reduction in (p)Ser^{265} signal in WT HFD arteries compared with ct. However, differences in (p)Ser^{265} signal were not observed in either AKAP150$^{-/-}$ HFD or ΔPIX HFD arteries compared with the respective ct. These findings suggest that NFATc3 is activated in WT HFD arterial myocytes, and anchoring of CaN by AKAP150 is a molecular prerequisite of NFATc3 activation under hyperglycemic conditions and diabetes mellitus.

Based on these findings, we investigated BK_{Ca} channel P_o in arterial myocytes isolated from WT and NFATc3-null (NFATc3$^{-/-}$) mice maintained in normal (10 mmol/L) and elevated (20 mmol/L) D-glucose. Although a reduction in channel P_o was observed in WT myocytes maintained in elevated D-glucose, BK_{Ca} P_o and α and β1 subunit expression was similar between NFATc3$^{-/-}$ arteries maintained in low and elevated glucose (Figure 6C and 6D). Together, these results suggest that the AKAP150/CaN signaling complex is required for NFATc3 activation, leading to BK_{Ca} impairment during hyperglycemia and diabetes mellitus.

Loss of AKAP150-Anchored CaN Attenuates HFD-Induced Increases in Blood Pressure

We performed telemetric blood pressure measurements in WT, AKAP150$^{-/-}$ and ΔPIX ct and HFD animals. Figure 7A shows representative blood pressure waveforms for WT ct and HFD mice. Consistent with previous studies,[24,25] WT HFD mice exhibited a significant increase in mean arterial pressure compared with ct (Online Table I). However, increases in blood pressure associated with HFD were significantly attenuated in both AKAP150$^{-/-}$ (≈60%) and ΔPIX (≈40%) mice compared with WT mice (Figure 7B; P<0.05). These data are consistent with the concept that AKAP150-anchored CaN contributes to impaired regulation of blood pressure during diabetes mellitus.

Discussion

In this study, we define a signaling pathway for the down-regulation of BK_{Ca} channel function, leading to enhanced vascular tone during noninsulin-dependent type 2 diabetes mellitus. In this pathway, anchoring of the Ca^{2+}/calmodulin-dependent phosphatase CaN by AKAP150 is a central mediator of glucose-induced NFATc3 activation and transcriptional

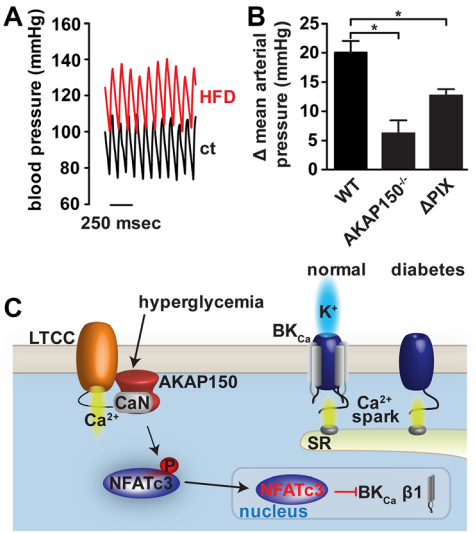

Figure 7. Ablation of A-kinase anchoring protein 150 (AKAP150) or disruption of the interaction between calcineurin (CaN) and AKAP150 attenuates high-fat diet (HFD)–induced elevation of blood pressure. **A**, Representative telemetric blood pressure waveforms for wild-type (WT) control (ct) and HFD mice. **B**, Bar plot of the change in mean arterial pressure for HFD vs corresponding ct for WT, AKAP150$^{-/-}$, and AKAP150 lacking binding site for calcineurin (ΔPIX) mice (n=3 animals per condition; *P<0.05). **C**, Proposed model for AKAP150-dependent suppression of large-conductance Ca^{2+}-activated K^+ (BK_{Ca}) channels in arterial myocytes during hyperglycemia and diabetes mellitus.

suppression of regulatory BK_{Ca} β1 subunits during diabetes mellitus. This ultimately produces a reduction in Ca^{2+} sensitivity of BK_{Ca} channel activation and promotes enhanced vascular tone under hyperglycemic conditions and diabetes mellitus (Figure 7C). Our findings demonstrate that genetic ablation of AKAP150 or selective perturbation of AKAP150–CaN interaction prevents suppression of BK_{Ca} channel function and β1 subunit expression and attenuates increases in blood pressure in diabetic animals.

The most intriguing observation in this study is the contribution of AKAP150-anchored CaN in the modulation of molecular signaling events that promote vascular remodeling associated with suppression of BK_{Ca} β1 subunits under hyperglycemic conditions and diabetes mellitus. The significance of localized phosphatase signaling in physiology has also been underscored by recent findings of an important role for AKAP150-targeted CaN signaling in insulin secretion by pancreatic β-cells[26] and synaptic incorporation of α-amino-3-hydroxy-5-methyl-4-isoxazolepropionic acid receptors in hippocampal neurons.[16] Compartmentalization of CaN through its association with AKAP150 is considered to have 2 effects on local phosphatase activity. Phosphatase anchoring can concentrate signals at precise subcellular locations to facilitate the selective dephosphorylation of substrates, or alternatively, precise sequestering of the phosphatase provides a means to segregate the action of this multifunctional enzyme.[27] Consistent with a crucial role for AKAP150-tethered CaN, disruption of the interaction between these 2 proteins was sufficient to prevent NFATc3 dephosphorylation and nuclear translocation, suppression of BK_{Ca} β1 subunit expression and channel function, and enhanced vascular tone in diabetic mice. Whether targeting of NFATc3 or other CaN substrates to specific subcellular compartments is part of this process is unclear. Regardless, the aforementioned data correlate with attenuation of an elevation in blood pressure in $AKAP150^{-/-}$ and ΔPIX HFD mice, presumably via a reduction in peripheral vascular resistance. However, although heart rate was not different between groups (Online Table I), we speculate that changes in cardiac output in WT HFD animals may also participate in the modulation of blood pressure. Future echocardiographic experiments will be important to address potential changes in heart function in WT, $AKAP150^{-/-}$, and ΔPIX HFD mice during diabetes mellitus.

The effects of disrupting AKAP150–CaN interaction on BK_{Ca} suppression were similar to pharmacological inhibition of CaN with CsA. Note that application of CsA is known to increase basal LTCC activity in arterial myocytes by preventing CaN-mediated feedback of protein kinase C-α activation of L-type Ca^{2+} channels.[28] Yet, in the presence of CsA, an increase in LTCC activity fails to promote NFATc3 activation. Accordingly, we have recently demonstrated that CsA prevents nuclear accumulation of NFATc3 but not the LTCC-dependent rise in $[Ca]^{2+}_i$ on protein kinase C-α activation.[6] Together, these findings suggest that inhibition of BK_{Ca} channel downregulation in the presence of CsA is because of inhibition of CaN /NFAT signaling rather than a reduction in Ca^{2+} influx. Given that AKAP150 also interacts with the C termini of LTCCs,[9] this scaffolding protein may function to position CaN near Ca^{2+} microdomain regions formed by high-activity LTCCs (Figure 7C). Consistent with this idea, LTCC-mediated NFATc3 translocation in arterial myocytes is insensitive to buffering bulk cytoplasmic Ca^{2+}, suggesting that the CaN/NFATc3 pathway is preferentially activated in arterial myocytes by microdomain Ca^{2+} gradients rather than global elevation of cytosolic Ca^{2+}.[6]

Although previous data suggest that activation of an AKAP-dependent pathway is necessary for increased LTCC activity during sustained hyperglycemic stimulation and diabetes mellitus,[5] the molecular identity of the AKAP involved in this process is currently unknown. Thus, it is possible that AKAP150-dependent post-translational modifications (eg, channel phosphorylation) together with suppression of BK_{Ca} channel function could concomitantly upregulate LTCC activity to contribute to enhanced vasoconstriction and vascular dysfunction during diabetes mellitus. Whether AKAP150 can also directly influence V_M of arterial myocytes in this process remains unclear. Previous studies have demonstrated that genetic ablation of AKAP150 reduces basal persistent LTCC activity under voltage clamp conditions,[29] suggesting that this scaffold could influence arterial myocyte $[Ca^{2+}]_i$ independent of changes in V_M.[19] Thus, the finding that IbTx inhibition of BK_{Ca} channels, which are less active at hyperpolarized V_M, induces a robust constriction in $AKAP150^{-/-}$ arteries suggests that $AKAP150^{-/-}$ arterial myocyte V_M is within the range in which BK_{Ca} channels act to oppose vasoconstriction.

The CaN/NFATc3 pathway of transcriptional regulation has been proposed as a metabolic sensor in vascular smooth muscle via detection of elevated extracellular glucose.[30] Taking into consideration that activation of NFATc3 is an absolute requirement for BK_{Ca} channel suppression during diabetes mellitus, the time course of β1 downregulation may closely follow that of the relationship between extracellular glucose and NFATc3 nuclear translocation. A previous report has found that significant NFATc3 nuclear accumulation begins as early as 8 minutes after exposure to elevated glucose in smooth muscle cells of intact cerebral arteries.[30] Thus, it is conceivable that downregulation of the BK_{Ca} β1 subunit may be initiated at this time point during sustained hyperglycemia. However, this process may occur more slowly in vivo, given the highly dynamic nature of NFATc3 nuclear import/export rate[31] and nonfasting plasma glucose levels in diabetic animals. Furthermore, the AKAP150/CaN/NFATc3 axis may be critical for pathophysiological induction or suppression of several other genes in smooth muscle. For instance, NFATc3 has been linked to downregulation of the gene encoding the voltage-dependent potassium channel $K_V2.1$,[11] increased expression of the contractile protein α-actin, vascular smooth muscle cell proliferation, and increased arterial wall thickness.[32] Thus, our data render plausible the concept that AKAP150-anchored CaN may be a key molecular event underlying NFATc3-dependent transcriptional regulation in smooth muscle, thus contributing to pathological vascular complications in the diabetic population.

Suppression of smooth muscle β1 subunits in response to elevated glucose in WT HFD mice is unlikely to be mediated by differential inflammatory response because it has previously been shown that systemic inflammation occurs at later stages (>35 weeks) of diet-induced obesity.[18,33] Yet, despite

this, additional signals could also contribute to NFATc3 activation[30,34] and β1 downregulation in response to elevated glucose in smooth muscle. For instance, $G_{q/11}$-coupled vasoactive compounds such as uridine triphosphate are released in response to high glucose. Nuclear translocation of NFATc3 in native arterial myocytes exposed to elevated extracellular glucose is sensitive to the ectonucleotidase apyrase and P2Y6 receptor antagonist MRS2578,[30] consistent with an additional role for nucleotide signaling in NFAT activation. In addition, recent reports have revealed a role for post-translational modifications, such as phosphorylation and oxidation, leading to decreased β1 protein levels and impaired BK_{Ca} channel activity after streptozotocin-induced type 1 diabetes mellitus.[35–37] In this model of type 1 diabetes mellitus, downregulation of coronary arterial smooth muscle BK_{Ca} β1 subunit has been linked to oxidative stress, causing an increase in ubiquitin ligase–dependent protein degradation. Although this mechanism has not yet been tested in experimental type 2 diabetes mellitus, it is conceivable that decreased mRNA/protein production and increased protein degradation may act in concert to reduce β1 function during hyperglycemia and diabetes mellitus. Note, however, that activation of additional pathways may vary between vascular beds and experimental models of diabetes. Future studies should determine whether transcriptional and post-translational mechanisms cooperatively act to impair BK_{Ca} channel function and expression during type 2 diabetes mellitus.

The proposed model of enhanced vascular tone in this study integrates systemic blood pressure measurements, biochemical data from small mesenteric arteries, as well as biophysical and functional studies in cerebral arterial myocytes. Therefore, our findings suggest a common mechanism (ie, anchored CaN-driven BK_{Ca} β1 subunit downregulation) of vascular dysfunction in the cerebral and mesenteric vasculature. We caution that although changes in BK_{Ca} channel function in cerebral arteries could alter cerebral blood flow and increase the probability of stroke during diabetes mellitus, they will have a limited effect on systemic blood pressure. Instead, downregulation of β1 in mesenteric arteries will likely have a larger influence on systemic blood pressure. In addition, although inhibition of CaN in the vasculature with CsA may prevent BK_{Ca} channel suppression during diabetes mellitus, this agent does not represent a beneficial therapeutic strategy, given that a well-known and seemingly paradoxical side effect of this drug is hypertension.[38,39] Although the causes of CsA-induced hypertension are multifactorial, renal sympathetic overactivity is a major contributing factor.[40,41] To circumvent this, our current study suggests that novel agents that selectively target vascular AKAP150–CaN interactions may be advantageous in preventing vascular K^+ channel remodeling while avoiding widespread effects of cell-wide CaN inhibition in the periphery.

Acknowledgments

We thank William A. Fayer and Kenneth Johnson for technical support, Dr Ye Chen-Izu for the use of the Olympus FV1000 confocal microscope, and Dr Johannes W. Hell for anti-$Ca_V1.2$ primary antibodies.

Sources of Funding

This work was supported by grants from the National Institutes of Health HL098200 (M.F. Navedo), HL07828 and HL086350-05 (M.A. Nystoriak), HL085686 and HL085870 (L.F. Santana), and NS040701, MH080291, and NS048154 (M.L. Dell'Acqua), American Heart Association grants 0735251N (M.F. Navedo) and 0840094N (L.F. Santana), and American Heart Association Western States Affiliate and the Lawrence J. and Florence A. DeGeorge Charitable Trust 13POST12730001 (M.A. Nystoriak).

Disclosures

None.

References

1. National high blood pressure education program working group report on hypertension in diabetes. *Hypertension*. 1994;23:145–158; discussion 159–160.
2. Barbagallo M, Shan J, Pang PK, Resnick LM. Glucose-induced alterations of cytosolic free calcium in cultured rat tail artery vascular smooth muscle cells. *J Clin Invest*. 1995;95:763–767.
3. Ungvari Z, Pacher P, Kecskemeti V, Papp G, Szollár L, Koller A. Increased myogenic tone in skeletal muscle arterioles of diabetic rats. Possible role of increased activity of smooth muscle Ca2+ channels and protein kinase C. *Cardiovasc Res*. 1999;43:1018–1028.
4. Navedo MF, Amberg GC, Votaw VS, Santana LF. Constitutively active L-type Ca2+ channels. *Proc Natl Acad Sci U S A*. 2005;102:11112–11117.
5. Navedo MF, Takeda Y, Nieves-Cintrón M, Molkentin JD, Santana LF. Elevated Ca2+ sparklet activity during acute hyperglycemia and diabetes in cerebral arterial smooth muscle cells. *Am J Physiol Cell Physiol*. 2010;298:C211–C220.
6. Nieves-Cintrón M, Amberg GC, Navedo MF, Molkentin JD, Santana LF. The control of Ca2+ influx and NFATc3 signaling in arterial smooth muscle during hypertension. *Proc Natl Acad Sci U S A*. 2008;105:15623–15628.
7. Gomez MF, Stevenson AS, Bonev AD, Hill-Eubanks DC, Nelson MT. Opposing actions of inositol 1,4,5-trisphosphate and ryanodine receptors on nuclear factor of activated T-cells regulation in smooth muscle. *J Biol Chem*. 2002;277:37756–37764.
8. Gao T, Yatani A, Dell'Acqua ML, Sako H, Green SA, Dascal N, Scott JD, Hosey MM. cAMP-dependent regulation of cardiac L-type Ca2+ channels requires membrane targeting of PKA and phosphorylation of channel subunits. *Neuron*. 1997;19:185–196.
9. Oliveria SF, Dell'Acqua ML, Sather WA. AKAP79/150 anchoring of calcineurin controls neuronal L-type Ca2+ channel activity and nuclear signaling. *Neuron*. 2007;55:261–275.
10. Li H, Pink MD, Murphy JG, Stein A, Dell'Acqua ML, Hogan PG. Balanced interactions of calcineurin with AKAP79 regulate Ca2+-calcineurin-NFAT signaling. *Nat Struct Mol Biol*. 2012;19:337–345.
11. Amberg GC, Rossow CF, Navedo MF, Santana LF. NFATc3 regulates Kv2.1 expression in arterial smooth muscle. *J Biol Chem*. 2004;279:47326–47334.
12. Nieves-Cintrón M, Amberg GC, Nichols CB, Molkentin JD, Santana LF. Activation of NFATc3 down-regulates the beta1 subunit of large conductance, calcium-activated K+ channels in arterial smooth muscle and contributes to hypertension. *J Biol Chem*. 2007;282:3231–3240.
13. Nelson MT, Patlak JB, Worley JF, Standen NB. Calcium channels, potassium channels, and voltage dependence of arterial smooth muscle tone. *Am J Physiol*. 1990;259:C3–C18.
14. Tanaka Y, Meera P, Song M, Knaus HG, Toro L. Molecular constituents of maxi KCa channels in human coronary smooth muscle: predominant alpha + beta subunit complexes. *J Physiol.* 1997;502(Pt 3):545–557.
15. Brenner R, Peréz GJ, Bonev AD, Eckman DM, Kosek JC, Wiler SW, Patterson AJ, Nelson MT, Aldrich RW. Vasoregulation by the beta1 subunit of the calcium-activated potassium channel. *Nature*. 2000;407:870–876.
16. Sanderson JL, Gorski JA, Gibson ES, Lam P, Freund RK, Chick WS, Dell'Acqua ML. AKAP150-anchored calcineurin regulates synaptic plasticity by limiting synaptic incorporation of Ca2+-permeable AMPA receptors. *J Neurosci.* 2012;32:15036–15052.
17. Surwit RS, Kuhn CM, Cochrane C, McCubbin JA, Feinglos MN. Diet-induced type II diabetes in C57BL/6J mice. *Diabetes*. 1988;37:1163–1167.
18. Winzell MS, Ahrén B. The high-fat diet-fed mouse: a model for studying mechanisms and treatment of impaired glucose tolerance and type 2 diabetes. *Diabetes*. 2004;53(Suppl 3):S215–S219.
19. Knot HJ, Nelson MT. Regulation of arterial diameter and wall [Ca2+] in cerebral arteries of rat by membrane potential and intravascular pressure. *J Physiol.* 1998;508(Pt 1):199–209.

20. Jaggar JH, Porter VA, Lederer WJ, Nelson MT. Calcium sparks in smooth muscle. *Am J Physiol Cell Physiol*. 2000;278:C235–C256.
21. Dick GM, Sanders KM. (Xeno)estrogen sensitivity of smooth muscle BK channels conferred by the regulatory beta1 subunit: a study of beta1 knockout mice. *J Biol Chem*. 2001;276:44835–44840.
22. Dell'Acqua ML, Dodge KL, Tavalin SJ, Scott JD. Mapping the protein phosphatase-2B anchoring site on AKAP79. Binding and inhibition of phosphatase activity are mediated by residues 315-360. *J Biol Chem*. 2002;277:48796–48802.
23. Okamura H, Aramburu J, García-Rodríguez C, Viola JP, Raghavan A, Tahiliani M, Zhang X, Qin J, Hogan PG, Rao A. Concerted dephosphorylation of the transcription factor NFAT1 induces a conformational switch that regulates transcriptional activity. *Mol Cell*. 2000;6:539–550.
24. Rahmouni K, Morgan DA, Morgan GM, Mark AL, Haynes WG. Role of selective leptin resistance in diet-induced obesity hypertension. *Diabetes*. 2005;54:2012–2018.
25. Mills E, Kuhn CM, Feinglos MN, Surwit R. Hypertension in CB57BL/6J mouse model of non-insulin-dependent diabetes mellitus. *Am J Physiol*. 1993;264:R73–R78.
26. Hinke SA, Navedo MF, Ulman A, Whiting JL, Nygren PJ, Tian G, Jimenez-Caliani AJ, Langeberg LK, Cirulli V, Tengholm A, Dell'Acqua ML, Santana LF, Scott JD. Anchored phosphatases modulate glucose homeostasis. *EMBO J*. 2012;31:3991–4004.
27. Tunquist BJ, Hoshi N, Guire ES, Zhang F, Mullendorff K, Langeberg LK, Raber J, Scott JD. Loss of AKAP150 perturbs distinct neuronal processes in mice. *Proc Natl Acad Sci U S A*. 2008;105:12557–12562.
28. Navedo MF, Amberg GC, Nieves M, Molkentin JD, Santana LF. Mechanisms underlying heterogeneous Ca2+ sparklet activity in arterial smooth muscle. *J Gen Physiol*. 2006;127:611–622.
29. Navedo MF, Nieves-Cintrón M, Amberg GC, Yuan C, Votaw VS, Lederer WJ, McKnight GS, Santana LF. AKAP150 is required for stuttering persistent Ca2+ sparklets and angiotensin II-induced hypertension. *Circ Res*. 2008;102:e1–e11.
30. Nilsson J, Nilsson LM, Chen YW, Molkentin JD, Erlinge D, Gomez MF. High glucose activates nuclear factor of activated T cells in native vascular smooth muscle. *Arterioscler Thromb Vasc Biol*. 2006;26:794–800.
31. Gomez MF, Bosc LV, Stevenson AS, Wilkerson MK, Hill-Eubanks DC, Nelson MT. Constitutively elevated nuclear export activity opposes Ca2+-dependent NFATc3 nuclear accumulation in vascular smooth muscle: role of JNK2 and Crm-1. *J Biol Chem*. 2003;278:46847–46853.
32. de Frutos S, Caldwell E, Nitta CH, Kanagy NL, Wang J, Wang W, Walker MK, Gonzalez Bosc LV. NFATc3 contributes to intermittent hypoxia-induced arterial remodeling in mice. *Am J Physiol Heart Circ Physiol*. 2010;299:H356–H363.
33. Kim F, Pham M, Maloney E, Rizzo NO, Morton GJ, Wisse BE, Kirk EA, Chait A, Schwartz MW. Vascular inflammation, insulin resistance, and reduced nitric oxide production precede the onset of peripheral insulin resistance. *Arterioscler Thromb Vasc Biol*. 2008;28:1982–1988.
34. Nilsson-Berglund LM, Zetterqvist AV, Nilsson-Ohman J, Sigvardsson M, González Bosc LV, Smith ML, Salehi A, Agardh E, Fredrikson GN, Agardh CD, Nilsson J, Wamhoff BR, Hultgårdh-Nilsson A, Gomez MF. Nuclear factor of activated T cells regulates osteopontin expression in arterial smooth muscle in response to diabetes-induced hyperglycemia. *Arterioscler Thromb Vasc Biol*. 2010;30:218–224.
35. Lu T, Zhang DM, Wang XL, He T, Wang RX, Chai Q, Katusic ZS, Lee HC. Regulation of coronary arterial BK channels by caveolae-mediated angiotensin II signaling in diabetes mellitus. *Circ Res*. 2010;106:1164–1173.
36. Zhang DM, He T, Katusic ZS, Lee HC, Lu T. Muscle-specific f-box only proteins facilitate bk channel β(1) subunit downregulation in vascular smooth muscle cells of diabetes mellitus. *Circ Res*. 2010;107:1454–1459.
37. Lu T, Chai Q, Yu L, d'Uscio LV, Katusic ZS, He T, Lee HC. Reactive oxygen species signaling facilitates FOXO-3a/FBXO-dependent vascular BK channel β1 subunit degradation in diabetic mice. *Diabetes*. 2012;61:1860–1868.
38. Lamb FS, Webb RC. Cyclosporine augments reactivity of isolated blood vessels. *Life Sci*. 1987;40:2571–2578.
39. Robert N, Wong GW, Wright JM. Effect of cyclosporine on blood pressure. *Cochrane Database Syst Rev*. 2010:CD007893.
40. Lyson T, McMullan DM, Ermel LD, Morgan BJ, Victor RG. Mechanism of cyclosporine-induced sympathetic activation and acute hypertension in rats. *Hypertension*. 1994;23:667–675.
41. Zhang W, Li JL, Hosaka M, Janz R, Shelton JM, Albright GM, Richardson JA, Südhof TC, Victor RG. Cyclosporine A-induced hypertension involves synapsin in renal sensory nerve endings. *Proc Natl Acad Sci U S A*. 2000;97:9765–9770.

Novelty and Significance

What Is Known?

- In the resistance vasculature, activation of large-conductance Ca^{2+}-activated K^+ (BK_{Ca}) channels opposes vasoconstriction; however, their activity is suppressed during diabetes mellitus, leading to enhanced vascular tone.
- Expression of BK_{Ca} β1 subunits, which confer Ca^{2+} and voltage sensitivity to the channel, is modulated by activation of the Ca^{2+}/calmodulin-dependent phosphatase calcineurin (CaN) and the transcription factor nuclear factor of activated T-cells c3 isoform (NFATc3) in arterial myocytes.
- The scaffolding protein A-kinase anchoring protein 150 (AKAP150) is a key regulator of CaN.

What New Information Does This Article Contribute?

- Under hyperglycemic conditions and in an experimental animal model of type 2 diabetes mellitus, activation of the CaN/NFATc3 pathway leads to transcriptional suppression of BK_{Ca} β1 subunits, which results in reduced BK_{Ca} channel function and enhanced vascular tone.
- AKAP150 is required for activation of the CaN/NFATc3 pathway and suppression of BK_{Ca} channel function and β1 expression in arterial myocytes of diabetic animals.
- Selective disruption of the interaction between AKAP150 and CaN prevents activation of NFATc3, BK_{Ca} β1 suppression, and enhanced vascular tone and attenuates increases in mean arterial blood pressure in diabetic animals.

Vascular complications are a major cause of death and disability in the diabetic population. Elevated blood pressure and reduced blood flow during diabetes mellitus result, in part, from enhanced contractility of arterial myocytes in the resistance vasculature, yet the contributing mechanisms are not well understood. Here, we establish the scaffolding protein AKAP150 as a critical mediator of transcriptional remodeling in arterial myocytes, leading to enhanced vascular tone during diabetes mellitus. Our findings demonstrate that AKAP150-dependent anchoring of the phosphatase CaN is a key molecular determinant of NFATc3 activation and downstream BK_{Ca} β1 suppression under hyperglycemic conditions and diabetes mellitus. Disrupting the interaction between AKAP150 and CaN is as sufficient in preventing BK_{Ca} channel remodeling under hyperglycemic conditions as cell-wide inhibition of CaN with cyclosporine A or genetic ablation of NFATc3. Our current study highlights the significance of compartmentalized phosphatase signaling in cardiovascular biology. Furthermore, it suggests broad importance of AKAP150-CaN in the pathophysiological induction of chronic remodeling during diabetic vascular dysfunction and as a novel target for therapeutic intervention.

Supplemental Material

Detailed methods

Animals: Wild type (C57Bl/6J, BalbC), AKAP150$^{-/-}$ (C57Bl/6J), NFATc3$^{-/-}$ (BalbC), and knock-in mice expressing AKAP150 lacking its CaN binding site (ΔPIX)[1] were euthanized by intraperitoneal injection of sodium pentobarbital (250 mg/kg), as approved by the University of California, Davis Institutional Animal Care and Use Committee. Mice were placed on either a low fat (10% kcal; ct) or high fat (60% kcal) diet (Research Diets) at 5 weeks of age and were sustained for 24-26 weeks. The composition of these diets and the propensity of mice maintained on this high fat diet to develop type 2 diabetes has been well described previously[2, 3]. Cerebral arteries were used for functional experiments (i.e. arterial diameter and electrophysiology), while mesenteric arteries were used for molecular biology experiments that required larger tissue input (i.e. Western blots, phosphatase assay, qPCR), and NFATc3 translocation experiments. For some experiments, arteries were acutely isolated from WT ct mice (5 weeks of age, ct diet) and organ cultured by placing arteries in serum-free DMEM-F12 culture media (Thermo Scientific) and incubating at 37 °C and 5% CO_2 for 48 hours. Arterial myocytes were dissociated from these arteries using enzymatic digestion techniques described previously[4, 5]. Cells were maintained in ice-cold nominally Ca^{2+}-free Ringer's solution until use.

Arterial diameter measurements: Freshly isolated posterior cerebral arteries were cannulated on glass micropipettes mounted in a 5 mL myograph chamber (University of Vermont Instrumentation and Model Facility) as described previously[6]. To allow for equilibration, arteries were pressurized to 20 mmHg and continuously superfused (37°C, 30 min, 3-5 mL/min) with physiological saline solution consisting of (in mmol/L) 119 NaCl, 4.7 KCl, 2 $CaCl_2$, 24 $NaHCO_3$, 1.2 KH_2PO_4, 1.2 $MgSO_4$, 0.023 ethylenediaminetetraacetic acid (EDTA), 11 D-glucose aerated with 5% CO_2/95% O_2. Bath pH was closely monitored and maintained at 7.35-7.40. Following equilibration period, intravascular pressure was increased to 60 mmHg and arteries were allowed to develop myogenic tone. Arteries not exhibiting stable myogenic tone after ~1 hour were discarded. To assess contribution of BK_{Ca} function to regulation of myogenic tone, the BK_{Ca} inhibitor iberiotoxin (IbTx; 100 nmol/L) was added to the superfusate. Arterial tone data is presented as a percent decrease in diameter relative to the maximum passive diameter at 60 mmHg obtained at the end of each experiment using Ca^{2+}-free saline solution containing nifedipine (1 µmol/L).

Electrophysiology: Single BK_{Ca} channel currents were recorded from inside-out membrane patches obtained from freshly dissociated cerebral arterial myocytes. Bath and pipette solutions contained (in mmol/L) 140 KCl, 1 HEDTA, and 10 HEPES, adjusted to pH 7.3. MaxChelator software was used to determine the amount of $CaCl_2$ needed to achieve the desired free Ca^{2+} concentration in the bath solution. Single channel currents were digitized at 5 kHz using pClamp 10 software (Axon Instruments Inc.). Data were filtered at 1 kHz using a Bessel filter (8 pole). Single channel openings were detected using the half-amplitude algorithm and data were analyzed (channel number, conductance, and P_o) using Clampfit (Axon Instruments Inc.). Only recordings with stable P_o values for a minimum of 2 minutes were analyzed. To calculate the P_o for a given recording, we estimated the number of BK_{Ca} channels per patch while patches were held at +80 mV in the presence of 10 µmol/L Ca^{2+} to maximize channel P_o [7]. All single-channel traces are representative of the mean P_o value calculated from multiple patches.

In some experiments, HEK293 cells were grown as described previously[8]. Cells were transfected with the BK_{Ca} α subunit and EGFP or co-transfected with BK_{Ca} α + β1 subunits in a 1:1 mix and EGFP (kindly provided by Dr. Heike Wulff, University of California, Davis, and Dr. Ligia Toro, University of California, Los Angeles) using PolyPlus jetPRIME following the manufacturer instructions. Cells were subcultured on glass coverslips for electrophysiological experiments 24 hrs after transfection. Single BK_{Ca} channel currents were recorded from inside-out membrane patches of cells exhibiting EGFP fluorescence, as described above.

Open time histograms were constructed in the Clampfit 10 module of pClamp 10. Curve fits were performed as described previously by our group[9] using a log-normal probability density function (PDF):

$$y = A \cdot e^{\frac{-\{[\ln(x)-\ln(\tau_1)]^2\}}{2\sigma_1^2}} + B \cdot e^{\frac{-/[\ln(x)-\ln(\tau_2)]^2}{2\sigma_2^2}}$$

where A and B are constants, t_1 is the short time constant, t_2 is the long time constant, and σ_1 and σ_2 are the standard deviations of t_1 and t_2, respectively. Dashed lines are individual fits for short (t_1) and long (t_2) opening. This analysis was validated by using an Akaike's Information Criterion, which determines the probability that a data set could be described by a particular set of competing models[10]. R^2 was used to assess the goodness of the fits.

Whole cell K^+ currents were measured using the conventional whole-cell patch clamp technique with an Axopatch 200B amplifier from freshly dissociated cerebral arterial myocytes. Currents were evoked by 1 sec depolarizing pulses from a holding potential of -70 mV to +60 mV in increments of 10 mV. K^+ currents were recorded before and after application of the BK_{Ca} channel blocker IbTx (100 nmol/L). IbTx-sensitive component was obtained by digital subtraction of traces recorded after exposure to IbTx from control traces. Bath solution consisted of the following components (in mmol/L): 130 NaCl, 5 KCl, 3 $MgCl_2$, 10 glucose, 10 HEPES, pH 7.4 with NaOH. Patch pipette solution was composed of (in mmol/L): 87 K-aspartate, 20 KCl, 1 $CaCl_2$, 1 $MgCl_2$, 5 MgATP, 10 EGTA, 10 HEPES, pH 7.2 with KOH. These conditions minimize the functional interaction between BK_{Ca} α and β1 subunits[11]. Experiments were carried out at room temperature. Electrophysiology recordings were analyzed using pCLAMP 10.

Ca^{2+} sparks imaging and analysis: Ca^{2+} sparks were imaged in cerebral arterial myocytes loaded with the Ca^{2+}-sensitive fluorescent indicator fluo-4-AM (5 μmol/L) using an Andor spinning disk confocal microscopy system coupled to an Olympus iX81 inverted microscope equipped with a 60x oil immersion lens (numerical aperture=1.49). Images were acquired at 100-200 Hz using Andor IQ software. Image analysis was performed using custom software (SparkLAB) written in LabVIEW language (National Instruments Corp.). Ca^{2+} sparks were identified using a computer algorithm similar to the one describe by Banyasz et al[12].

Western blot analysis and coimmunoprecipitation: Whole lysates were collected from cerebral and mesenteric arteries by sonication (20 min, 4°C) in a triton lysis buffer solution containing (in mmol/L) 150 NaCl, 10 Na_2HPO_4, 1 EDTA with 1% deoxycholic

acid, 1% sodium dodecyl sulfate and protease inhibitors (Complete Mini protease inhibitor cocktail, Roche). Tissue debris and nuclear fragments were removed by centrifugation at 10,000 rpm (10 min, 4°C) and whole cell lysates were obtained as the supernatant. An equal amount of protein was loaded for each tissue lysate. Proteins were separated under reducing conditions on a 4-20% polyacrilamide gel (Bio-Rad) by electrophoresis at 100 V for 1 hr and electrophoretically transferred to a polyvinylidene difluoride membrane at 100 V (1 hr, 4°C). Membranes were washed in tris-buffered saline with 0.1% tween 20 (TBS-t) and blocked with 10% nonfat milk in TBS-t (1 hr, room temperature). Membranes were then incubated with specific polyclonal antibodies against BK_{Ca} α (1:200; Alomone, APC-021), BK_{Ca} β1 (1:200; Abcam, Ab 3587), $Ca_V1.2$ (1:400; kindly provided by Dr. Johannes W. Hell from the University of California, Davis), p-NFATc3 serine 265 (1:200; Santa Cruz, sc-32982) NFATc3 residues 321-395 (1:200; Santa Cruz, sc-8321) overnight at 4°C or monoclonal antibody against β actin (1:5,000; Pierce, MA5-15739) prepared in TBS-t with 1% bovine serum albumin and 0.01% sodium azide (1 hr, room temperature). Membranes were then incubated (1 hr, room temperature) with horseradish peroxidase-labeled donkey anti-rabbit (1:5,000; Jackson ImmunoResearch, 711-035-152) or goat anti-mouse (1:5,000; Santa Cruz, sc-2005) in TBS-t containing 5% nonfat dried milk. Bands were identified by enhanced chemiluminescence and exposed to X-ray film. Densitometry for immunoreactive bands was performed with ImageJ software (National Institutes of Health) and density was expressed as a percentage of β actin for each lane. n values for densitometry data indicate number of animals.

For AKAP79/CaN coimmunoprecipitation experiments, HEK293A cells were transfected with pcDNA-2-Flag-AKAP79 (human ortholog of AKAP150), or a mutant of this construct (ΔPIX) lacking residues 337-343 (PIAIIIT; corresponding to residues 655-66 of AKAP150). 48 hours post-transfection, cells were lysed and harvested in 20 mmol/L HEPES, 150 mmol/L NaCl, and 1% Triton X-100. IP samples were supplemented with 5 µg calmodulin and 2 mmol/L $CaCl_2$. 2 µg mouse anti-Flag IgG (or control IgG) were added for one hour, after which 30 µL of protein A/G agarose slurry was added. After incubation for 1 hour, beads were washed three times with 1 mL lysis buffer (supplemented with 2 mmol/L $CaCl_2$), and eluted using SDS sample buffer. IP samples were analyzed by Western blot. Blots were blocked for one hour in 5% milk in TBS-t, washed 3 times for 5 min each in TBS-t and incubated overnight in primary antibody (M2 anti-Flag HRP, or anti-PP2B A subunit, Millipore). Blots were then washed 4 times for 5 minutes and then developed (for the anti-Flag HRP), or incubated in anti-rabbit HRP for 1 hour and subsequently washed and developed. Signals were quantified as the PP2B/Flag-AKAP79 signal ratio.

Quantitative polymerase chain reaction: Total RNA was isolated from cerebral and mesenteric arteries using an RNeasy Micro kit (Qiagen) and reverse transcribed to cDNA with the SuperScript First-Strand synthesis system (Invitrogen). Polymerase chain reaction was performed with primers detecting BK_{Ca} α (GenBank accession number NMOL/L_010610, sense nt 1204-1227 and antisense nt 1457-1478), BK β1 (GenBank accession number NMOL/L_031169.2; sense nt 604-627 and antisense nt 780-803). β actin was used as an internal control (GenBank accession number V01217; sense nt 2384-2404 and antisense nt 3071-3091). Amplification was performed using a Quantitect SYBR Green PCR mix (Qiagen) and a real-time PCR system (Applied Biosystems). Expression for each gene was normalized to β actin and expressed as a percentage of 5 mmol/L D-glucose controls.

Measurement of calcineurin and NFAT localization: Calcineurin activity was measured by using a colorimetric Calcineurin Cellular Activity Assay kit (Calbiochem, EMD Biosciences) following the manufacturer's instruction. For CsA-specificity analysis, HEK293A cells were transfected with pcDNA-V5-PP1c or YFP-PP2B (CaN). The phosphatases were coimmunoprecipitated as above, but in the presence or absence of 1 μmol/L CsA in the lysis and wash buffers. After 3 washes, the immunoprecipitates were washed in phosphatase activity buffers containing $CaCl_2$ and calmodulin, and then assayed for activity using a phospho-RII substrate and a malachite green dye detector of free phosphate. Immunoprecipitates from mock transfected HEK cells (pcDNA) were used as a control. Western blot analysis was performed on IP samples and 10 μg of sample input, using antibodies reactive against V5, YFP, or α tubulin.

NFATc3 localization was assessed using the Polyplus *in vivo* jetPEI method to deliver NFATc3 tagged with EGFP or only EGFP to smooth muscle cells. A 0.5 mL aliquot of a solution containing the jetPEI solution (2.8%) and NFATc3-EGFP or EGFP (100 μg total DNA each) was injected intraperitoneally in ct or HFD mice per manufacturer's instructions. After 4-5 days, mesenteric arteries were collected, individual myocytes were isolated and NFATc3-EGFP or EGFP fluorescence was evaluated. Isolated cells were used for these experiments to avoid the auto-fluorescence commonly detected in intact arteries. Dissociated cells were plated in a recording chamber and stained with Hoechst nuclear stain. NFATc3-EGFP or EGFP fluorescence, Hoechst and differential interference contrast images were obtained using an Olympus FV1000 confocal microscopy system on an Olympus iX81 microscope with a 60X water immersion lens (N.A. 1.4). Images were collected at multiple optical planes (z-axis step size = 1 μm). Gain and laser power parameters were first established using untransfected, freshly dissociated arterial myocytes (Online Figure X). During initial image acquisition of cells from injected mice, all available cells were examined. Based on these data, transfection efficiency using the jetPEI method was ~50%. However, because the goal was to determine the localization of NFATc3 in arterial myocytes from ct and HFD mice, only cells exhibiting fluorescence above the set parameters, obtained with untransfected myocytes, were analyzed. Fluorescence intensities were corrected for background signal. NFATc3 translocation was analyzed by calculating mean EGFP fluorescence intensities in the nucleus (F_{nuc}) and cytosol (F_{cyt}) and expressed as F_{nuc}/F_{cyt} ratio. Data were analyzed using ImageJ software.

Telemetric blood pressure measurements: Blood pressure was monitored in conscious adult WT, AKAP150$^{-/-}$ and ΔPIX mice maintained on either 10% kcal or 60% kcal diet using a telemetry system (Data Science International). Briefly, mice were anesthetized with isoflurane and a ventral midline incision from the lower mandible to the sternum was made to isolate the left common carotid artery. Two lengths of 7-0 silk sutures were threaded beneath the vessel for retraction and ligation. The artery was permanently ligated at the level of the bifurcation between the interior and exterior carotid arteries. The second suture was used to occlude blood flow temporarily to allow insertion of a catheter. A 25 gauge needle was used to make an incision in the artery through which the tip of the catheter was inserted. The catheter was advanced to the thoracic aorta and tied in place with the suture. A subcutaneous pocket was then made to place the transmitter body. After placement of the transmitter body, the incision was closed with 5-0 sutures.

Blood pressure was recorded continuously in conscious, freely moving mice and stored in the hard drive of a personal computer running Dataquest software (Data Science International). Control blood pressure measurements began 7 days after surgery to allow animals to recover. After this recovery period, blood pressures were recorded for 7-10 days.

Chemicals and Statistical analyses: All chemical reagents were from Sigma-Aldrich (St. Louis, MO) unless otherwise stated. Iberiotoxin was from Peptides International Inc. (Louisville, KY). Data are expressed as mean ± SEM. Data obtained using multiple vessels from the same animal were pooled for statistical analyses. Data were analyzed using GraphPad Prism software. Statistical significance was determined by Student's *t*-test or one-way analysis of variance followed by Tukey multiple comparison test for comparison of multiple groups. Statistical significance (denoted by * in figures) was considered at the level of $P<0.05$.

References

1. Sanderson JL, Gorski JA, Gibson ES, Lam P, Freund RK, Chick WS, Dell'Acqua ML. Akap150-anchored calcineurin regulates synaptic plasticity by limiting synaptic incorporation of ca2+-permeable ampa receptors. *J Neurosci*. 2012;32:15036-15052

2. Winzell MS, Ahren B. The high-fat diet-fed mouse: A model for studying mechanisms and treatment of impaired glucose tolerance and type 2 diabetes. *Diabetes*. 2004;53 Suppl 3:S215-219

3. Kim F, Pham M, Maloney E, Rizzo NO, Morton GJ, Wisse BE, Kirk EA, Chait A, Schwartz MW. Vascular inflammation, insulin resistance, and reduced nitric oxide production precede the onset of peripheral insulin resistance. *Arteriosclerosis, thrombosis, and vascular biology*. 2008;28:1982-1988

4. Amberg GC, Rossow CF, Navedo MF, Santana LF. Nfatc3 regulates kv2.1 expression in arterial smooth muscle. *J Biol Chem*. 2004;279:47326-47334

5. Nieves-Cintrón M, Amberg GC, Nichols CB, Molkentin JD, Santana LF. Activation of nfatc3 down-regulates the β1 subunit of large conductance, calcium-activated k^+ channels in arterial smooth muscle and contributes to hypertension. *J Biol Chem*. 2007;282:3231-3240

6. Amberg GC, Bonev AD, Rossow CF, Nelson MT, Santana LF. Modulation of the molecular composition of large conductance, ca^{2+} activated k^+ channels in vascular smooth muscle during hypertension. *J Clin Invest*. 2003;112:717-724

7. Meera P, Wallner M, Jiang Z, Toro L. A calcium switch for the functional coupling between alpha (hslo) and beta subunits (kv,cabeta) of maxi k channels. *FEBS letters*. 1996;385:127-128

8. Navedo MF, Cheng EP, Yuan C, Votaw S, Molkentin JD, Scott JD, Santana LF. Increased coupled gating of l-type ca2+ channels during hypertension and timothy syndrome. *Circulation research*. 2010;106:748-756

9. Navedo MF, Amberg GC, Westenbroek RE, Sinnegger-Brauns MJ, Catterall WA, Striessnig J, Santana LF. Cav1.3 channels produce persistent calcium sparklets, but cav1.2 channels are responsible for sparklets in mouse arterial smooth muscle. *Am J Physiol Heart Circ Physiol*. 2007;293:H1359-1370

10. Akaike H. A new look at the statistical model identification. *IEEE Trans. Autom. Control*. 1974;AC19:716–723

11. Meera P, Wallner M, Jiang Z, Toro L. A calcium switch for the functional coupling between alpha (hslo) and beta subunits (k_{v,ca_β}) of maxi k channels. *FEBS Lett*. 1996;385:127-128

12. Banyasz T, Chen-Izu Y, Balke CW, Izu LT. A new approach to the detection and statistical classification of ca2+ sparks. *Biophys J*. 2007;92:4458-4465

Online Figures

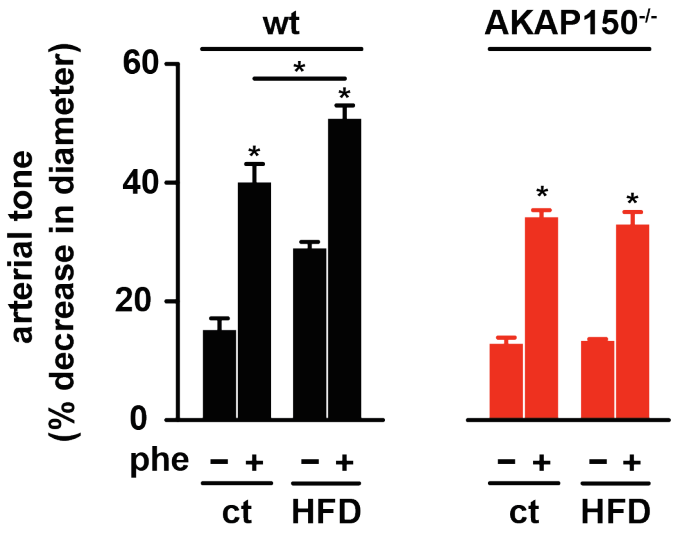

Online Figure I: Arteries from WT HFD mice exhibit robust constriction in the presence of phenylephrine. Bar plot summarizing arterial tone in the absence (-) and presence (+) of phenylephrine (phe; 1 μmol/L) in WT ct (n=8 from 5 animals), WT HFD (n=7 from 5 animals), AKAP150$^{-/-}$ ct (n=8 from 5 animals) and AKAP150$^{-/-}$ HFD (n=7 from 4 animals) arteries. *P < 0.05 for (+) phe vs. (-) phe groups, and WT HFD (+) phe vs. WT ct (+) phe groups.

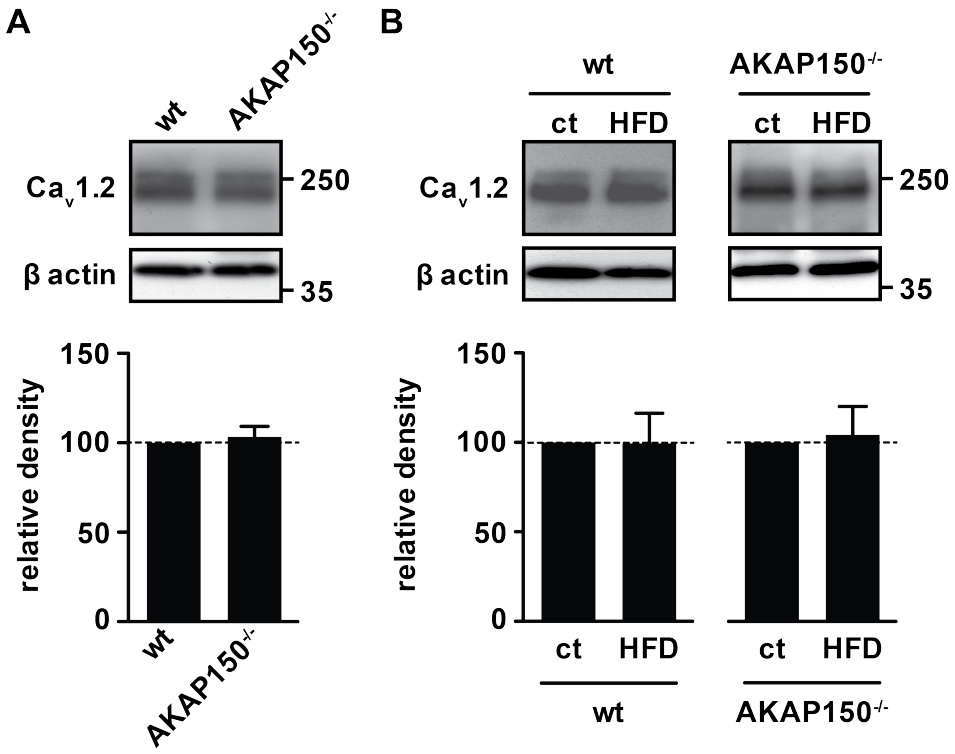

Online Figure II: L-type Ca^{2+} channel $Ca_V1.2$ subunit expression is similar between WT and AKAP150$^{-/-}$, and between ct and HFD arteries. ***A*** Representative Western blots corresponding to the $Ca_V1.2$ subunit and β actin (*upper panel*) and summary densitometric data (*bottom panel*) for WT and AKAP150$^{-/-}$ ct mesenteric arteries (n=3 lysates). ***B*** Representative Western blots corresponding to $Ca_V1.2$ and β actin (*upper panel*) and summary densitometric data (*bottom panel*) for WT ct and HFD (n=4 lysates) and AKAP150$^{-/-}$ ct and HFD (n=4 lysates) mesenteric arteries.

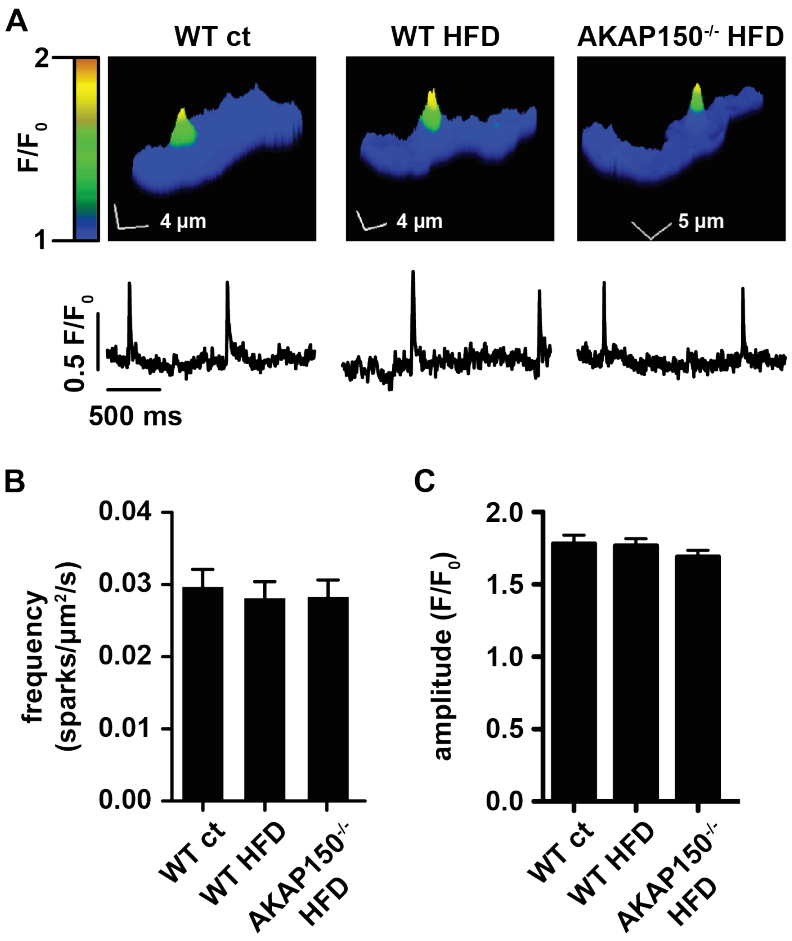

Online Figure III: Frequency and amplitude of Ca^{2+} sparks are similar in arterial myocytes from WT and AKAP150$^{-/-}$ HFD animals. ***A*** Representative three dimensional pseudo-color images of Ca^{2+} sparks and fractional fluorescence traces (F/F_o) in fluo-4-loaded cerebral arterial myocytes from WT ct, WT HFD and AKAP150$^{-/-}$ HFD mice. ***B, C*** Bar plot summarizing Ca^{2+} spark frequency (*B*) and amplitude (*C*) in WT ct, WT HFD and AKAP150$^{-/-}$ HFD arterial myocytes (n=35 cells for each group).

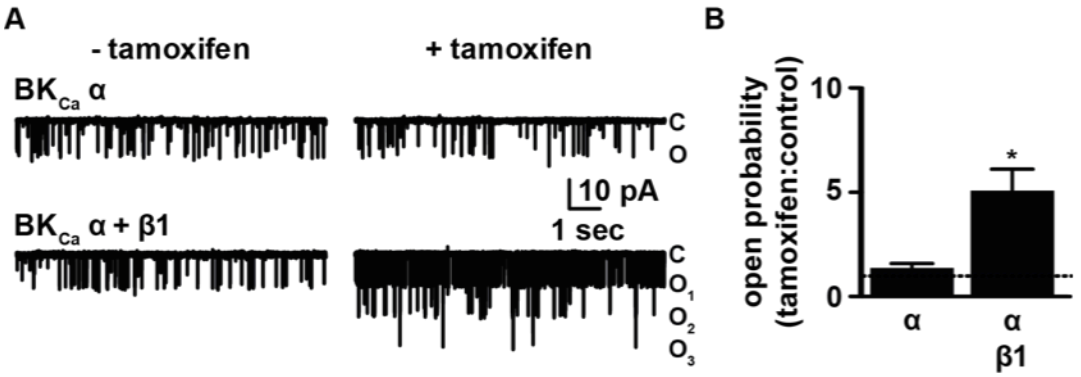

Online Figure IV: BK_{Ca} β1 expression is necessary for tamoxifen-induced activation of BK_{Ca} channels. ***A*** Representative single BK_{Ca} channel records at +40 mV and 1 µmol/L Ca^{2+} obtained from excised membrane patches of HEK293 cells expressing only BK_{Ca} α subunits or coexpressing BK_{Ca} α and β1 subunits in the absence and presence of the β1-selective BK_{Ca} channel activator tamoxifen (1 µmol/L) (C: closed; O: open). ***B*** Bar plot summarizing open probability (P_o; tamoxifen:control) for HEK293 cells expressing BK_{Ca} α (n=13 cells) and BK_{Ca} α+β1 (n=16 cells) subunits. Dashed lines represent P_0 (tamoxifen:control) = 1.

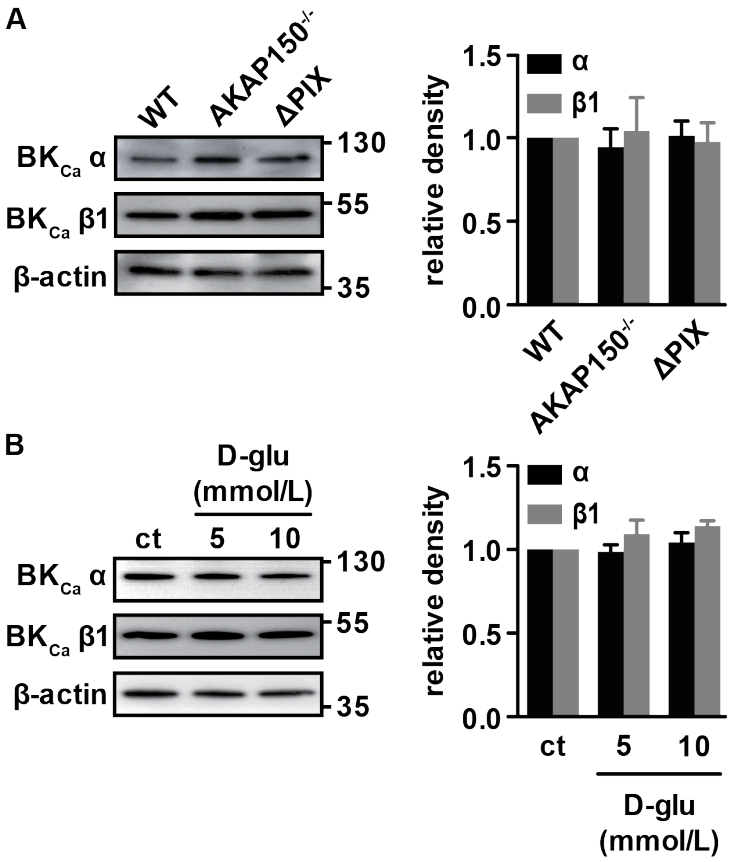

Online Figure V: Ablation of AKAP150, disruption of the interaction between AKAP150 and calcineurin, or organ culture in normoglycemic conditions does not alter basal expression of BK_{Ca} α and β1 subunits. ***A*** Representative Western blots showing BK_{Ca} α and β1 subunits, and β actin (*left*) and summary densitometric data (*right*) indicating relative basal α and β1 subunit expression in WT, AKAP150 and ΔPIX mesenteric arteries (n=3 lysates per condition). ***B*** Representative Western blots showing BK_{Ca} α and β1 subunits, and β actin (*left*) and summary densitometric data (*right*) indicating relative α and β1 subunit expression in freshly isolated arteries (ct) and arteries organ cultured (48 hrs) in 5 mM and 10 mM D-glucose (n=3 lysates per condition).

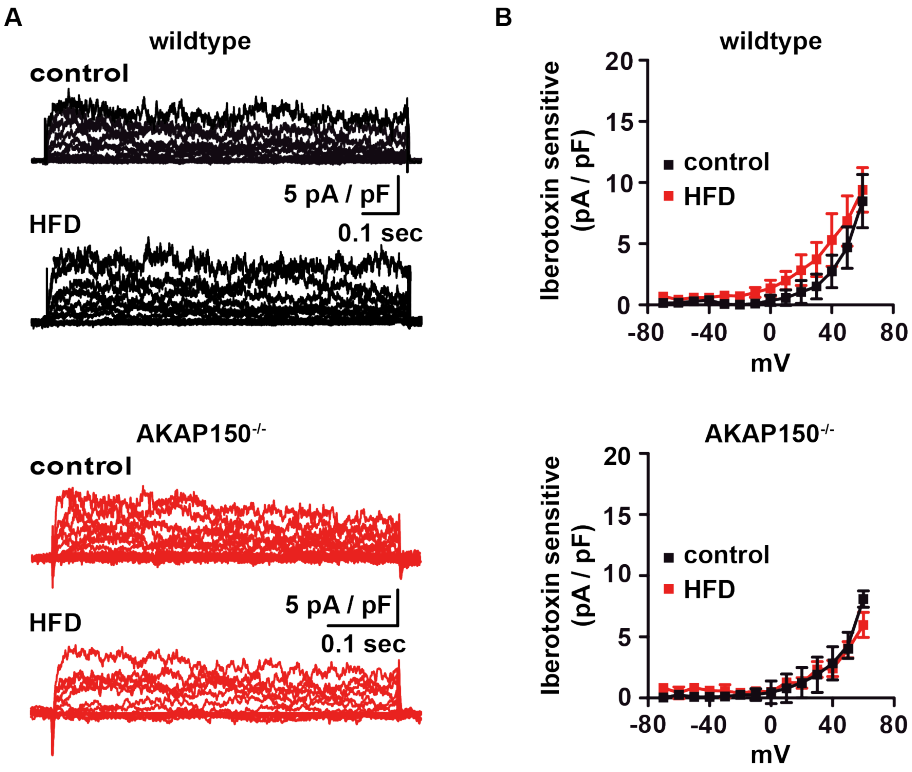

Online Figure VI: Whole cell I_{BK} in WT and AKAP150$^{-/-}$ ct and HFD arterial myocytes. ***A*** Representative families of IbTx-sensitive whole-cell currents (i.e. I_{BK}) recorded in cerebral artery myocytes from WT and AKAP150$^{-/-}$ ct and HFD mice. ***B*** I_{BK} current-voltage relationship in WT ct (n=7 from 4 animals) and HFD (n=6 from 4 animals), and AKAP150$^{-/-}$ ct (n=6 from 4 mice) and HFD (n=7 from 4 mice) myocytes. **P* < 0.05.

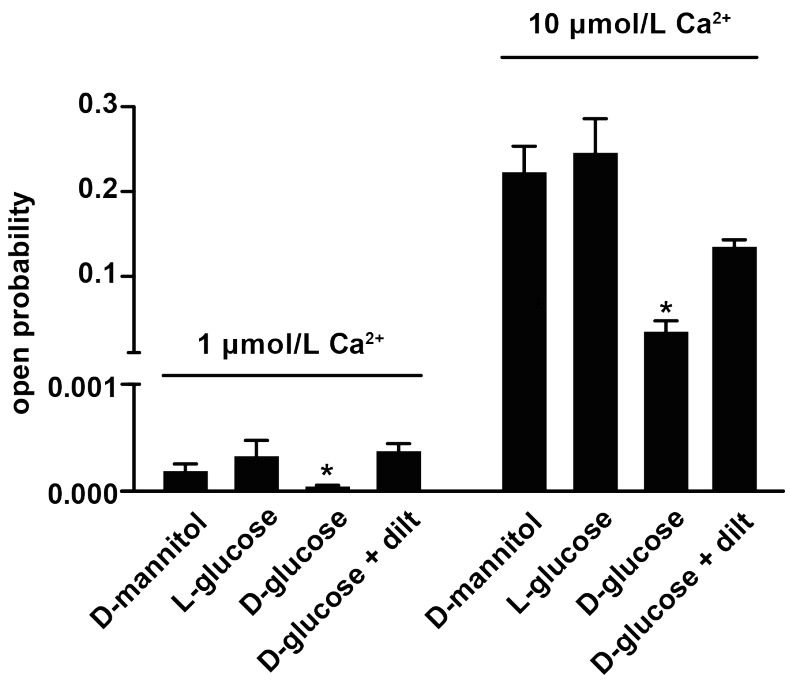

Online Figure VII: BK_{Ca} open probability is unaffected by osmolarity or non-metabolized glucose, and decreased channel activity in response to elevated D-glucose is blocked by diltiazem. Bar plot summarizing P_o of BK_{Ca} channels in myocytes from WT cerebral arteries incubated (48 hrs) in D-glucose (5 mmol/L)/D-mannitol (15 mmol/L) (n=10 cells), D-glucose (5mmol/L)/L-glucose (15 mmol/L) (n=8 cells), D-glucose (20 mmol/L; n=8 cells) or D-glucose (20 mmol/L) in the presence of diltiazem (50 µmol/L; n=7 cells) at indicated free Ca^{2+} concentrations. *$P < 0.05$.

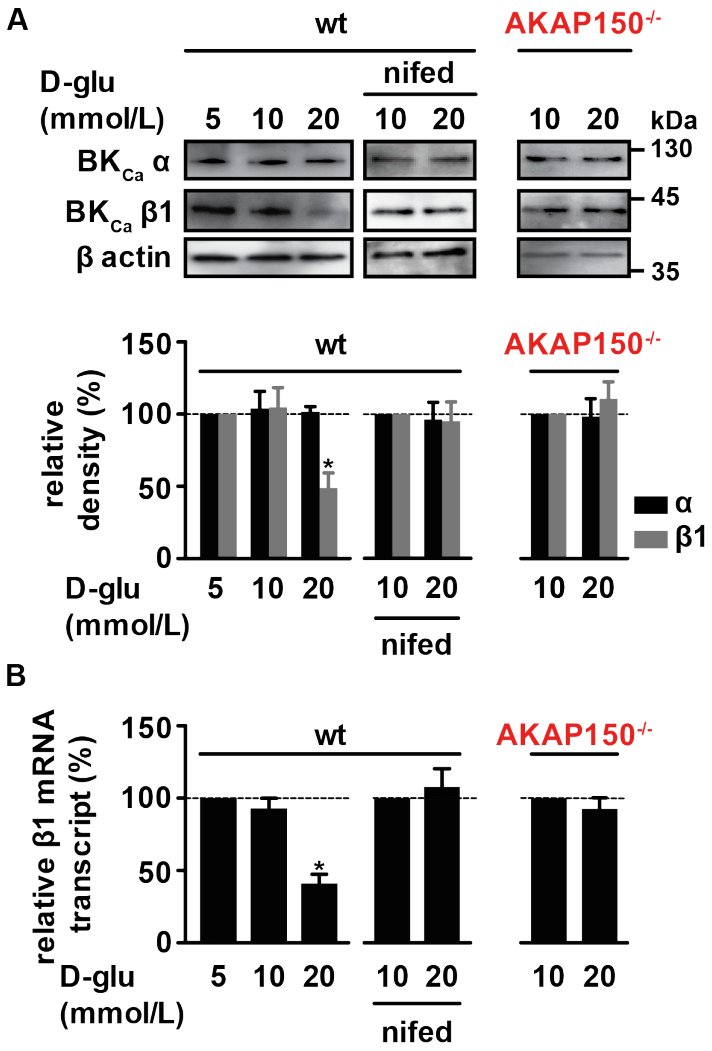

Online Figure VIII: Nifedipine and ablation of AKAP150 prevent decreased BK_{Ca} channel β1 subunit expression by elevated glucose. ***A*** Upper *panel:* Representative Western blots showing immunoreactive bands corresponding to BK_{Ca} α and β1 subunits and β actin for WT arteries in the absence and presence of nifedipine (1 μmol/L) and AKAP150$^{-/-}$ arteries incubated in the indicated D-glucose concentrations. *Lower panel:* Bar plots summarizing Western blot data for BK_{Ca} α and β1 protein in WT and AKAP150$^{-/-}$ mesenteric arteries incubated in the indicated D-glucose concentration, and in the absence and presence of nifedipine for WT arteries (n=3 lysates per condition). ***B*** Bar plots summarizing quantitative real-time PCR data for BK_{Ca} β1 transcript in WT and AKAP150$^{-/-}$ mesenteric arteries incubated in the indicated D-glucose concentration, and in the absence and presence of nifedipine (1 μmol/L) for WT arteries (n=3 lysates per condition). *$P < 0.05$.

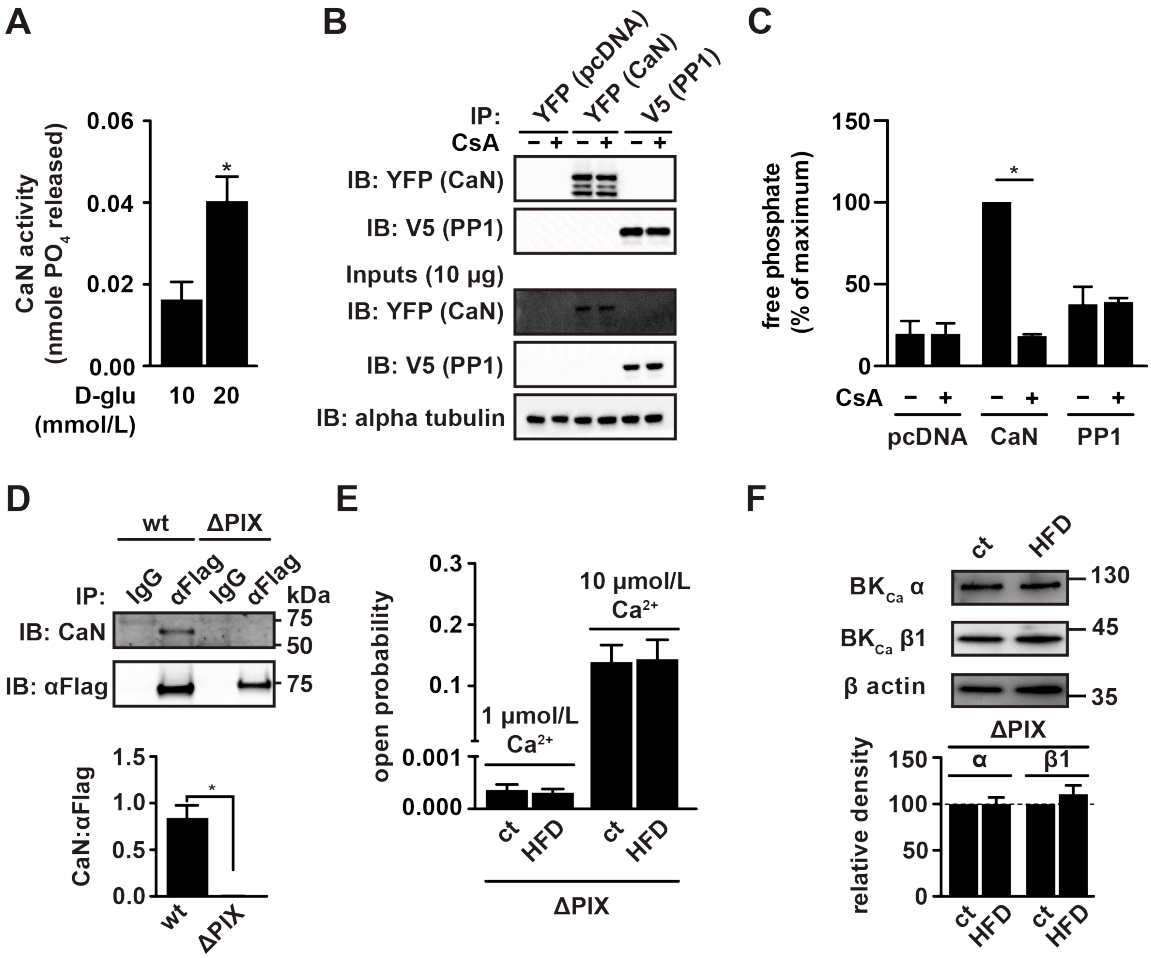

Online Figure IX: AKAP150/calcineurin interaction is necessary for suppression of BK_{Ca} channel function and downregulation of β1 expression in HFD mice. ***A*** Cellular CaN activity in WT mesenteric arteries incubated in 10 or 20 mmol/L D-glucose (n=3). ***B, C*** CsA inhibits CaN, but not PP1 activity against a phosphopeptide substrate. (*B*) Western blot analysis of co-immunoprecipitation experiments showing equal loading of controls and IP efficiency between untreated and CsA-treated (1 µmol/L) YFP-CaN, V5-PP1, and pcDNA samples. (*C*) Bar plot summarizing phosphatase activity of samples expressing pcDNA, CaN or PP1 in the presence or absence of CsA (n=3). Data was normalized to the peak values for each experiment. ***D*** Representative Western blot analysis (*top*) of immunoprecipitation of AKAP79 (αFlag) or a mutant lacking the PIAIIIT region (ΔPIX) followed by Western blot analysis to detect αFlag and CaN, and quantification of Western blot analyses (*bottom*; CaN:αFlag; n=3). ***E*** Bar plot summarizing P_o of BK_{Ca} channels recorded at -40 mV and indicated Ca^{2+} concentration in myocytes from ΔPIX ct (n=13 cells from 6 animals) and HFD (n=14 cells from 5 animals) mice. ***F*** Representative Western blots (*top*) and corresponding densitometric summary data (*bottom*) for BK_{Ca} α and β1 subunits in mesenteric arteries isolated from ΔPIX ct (n=5) and HFD mice (n=5). Protein levels for BK_{Ca} α and β1 were normalized to β actin and expressed as relative to control levels. **P* < 0.05.

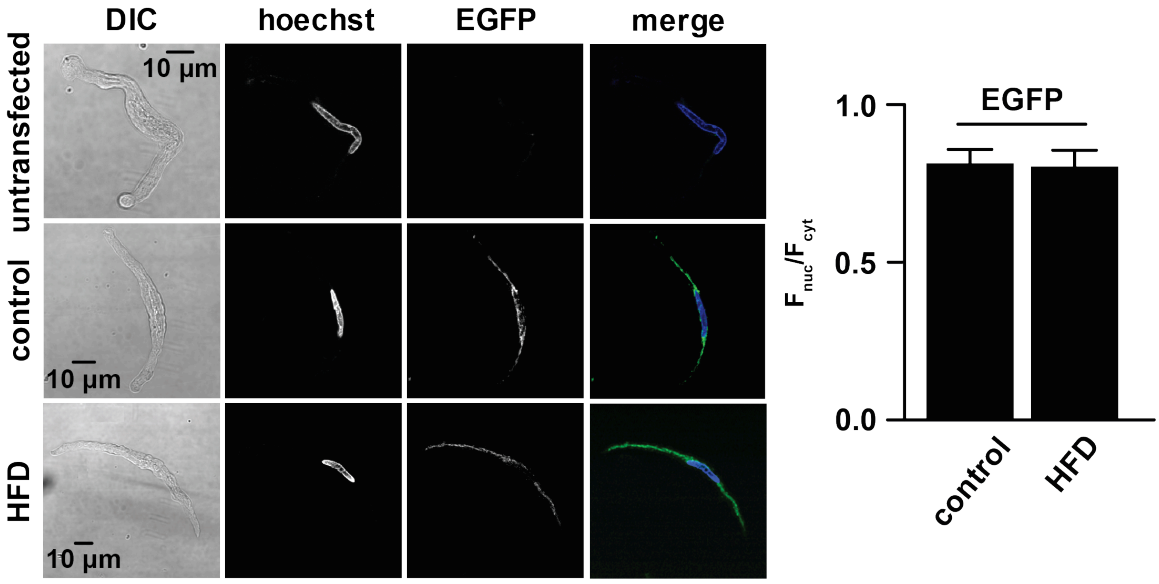

Online Figure X: Expression of EGFP in arterial myocytes from WT ct and HFD mice. ***A*** Transmitted light and background-corrected confocal images of an untransfected control mesenteric arterial myocyte, and ct and HFD WT mesenteric artery myocytes expressing EGFP. The nuclei were stained with hoechst. ***B*** Bar plot summarizing EGFP localization in mesenteric artery myocytes from WT control (n=48 cells) and HFD (n=49 cells) mice. Data is expressed as ratio of nuclear fluorescence (F_{nuc})/cytoplasmic fluorescence (F_{cyt}).

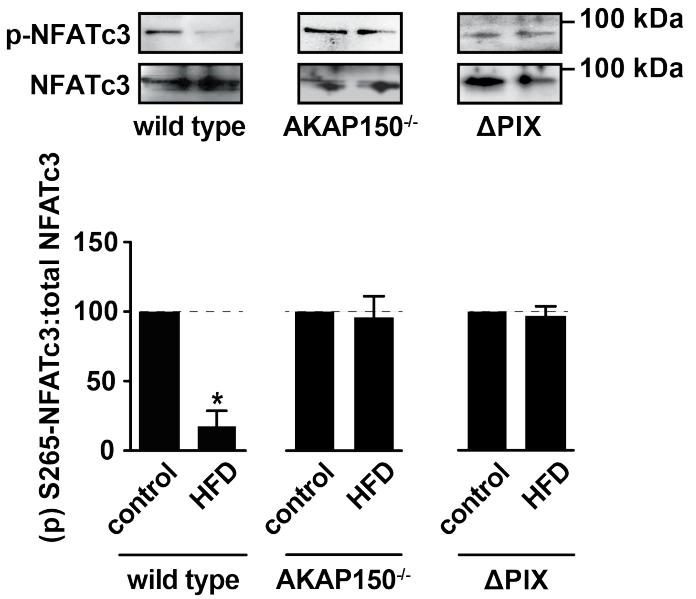

Online Figure XI: NFATc3 is significantly dephosphorylated in arteries from wild type, but not AKAP150$^{-/-}$ or ΔPIX HFD mice. Representative Western blots (*top*) and corresponding densitometric summary data (*bottom*) for (P)Ser^{265} (p-NFATc3) and total NFATc3 in control and HFD WT (n=5 lysates), AKAP150$^{-/-}$ (n=4 lysates), and ΔPIX (n=7 lysates) mice. Data are normalized to total NFATc3 and expressed as relative to corresponding controls for each genotype. *$P < 0.05$.

Online Table I: Body weight, non-fasting blood glucose and mean arterial blood pressure in wild type, AKAP150$^{-/-}$ and ΔPIX mice fed control and high fat diet.

	Body Weight (g)	Blood glucose (mmol/L)	Mean Arterial Blood Pressure (mmHg)	Heart Rate (BPM)
wild-type				
control	39 ± 1.7	9 ± 0.4	95 ± 5.1	604 ± 11.3
high fat diet	54 ± 1.1*	16.2 ± 1.4*	115 ± 2.0*	622 ± 5.9
AKAP150$^{-/-}$				
control	31 ± 0.3	8.7 ± 0.8	109 ± 1.6	571 ± 26.9
high fat diet	52 ± 2.9*	16.4 ± 1.6*	115 ± 2.2	629 ±19.2
ΔPIX				
control	32.4 ± 0.5	8.1 ± 0.5	106 ± 6.5	573 ± 48.0
high fat diet	50 ± 3.0*	15.7 ± 0.8*	119 ± 1.1	621 ± 5.7

Values are mean ± SEM obtained at 24-26 weeks after start of diet at 5 weeks of age. *P<0.05.